GEOCHEMISTRY OF THREE CASCADE VOLCANOES

by

David Howard Swenson

A Thesis Submitted to the Faculty of the
New Mexico Institute of Mining and Technology

In Partial Fullfillment of the Requirements
for the Degree of Master of Science
In Geochemistry

November 1973

TABLE OF CONTENTS

Page

LIST OF FIGURES

Figure Number | | Page

Figure Number | Page

LIST OF TABLES

ACKNOWLEDGEMENTS

I am very grateful to Dr. Condie, my advisor, for his constant enthusiasm and assistance. This study was made possible by Dr. Condie's NSF grant #GA-26390. I am also grateful to Dr. Billings and Dr. Chapin for their advice and critical reading of this manuscript. The field assistance given by David Hayslip, Josephy Cepeda, James Dodson, Charles O'Melveney and John Stirling is gratefully appreciated. I also appreciate the cooperation of the Chief Park Naturalist and his staff at Mount Rainier National Park for permitting the collection of samples and for their advice concerning cleavers that would be accessible for sampling. Dr. Walker is acknowledged for his assistance with the analytic work involved in this study. Also acknowledged is the assistance given by Dennis Umshler, Rod Woodcock, David Wright and Jerry Gagnepain in the preparation of samples.

ABSTRACT

Lava flows from the stratovolcanoes; Mount Shasta , Mount Jefferson and Mount Rainier, were sampled in detail and analyzed for Si, Ti, Al, Fe, Ca, Mg, Na, K, Rb, Sr, Cu, Zn, Ni and Co. Each volcano exhibit~~e~~s a distinct calc-alkaline composition. Chemical variation diagrams, in general, do not exhibit smooth nor continuous chemical trends as previously reported for these volcanoes. Chemical composition varies systematically only when compared in short (≈150 m) stratigraphic sections. Chemical unconformities in stratigraphic sections delineate sub-sequences of lava flows that originated from a common magma batch , therefore, suggesting that many magma batches are represented in the formation of a volcano. Chemical variations in stratigraphic sections generally are not accompanied by mineralogical variations. All three volcanoes are chiefly composed of uniform pyroxene andesites of the calc-alkaline series, however, Mount Shasta and Mount Rainier have final stages of volcanic activity that are represented by satellite cone eruptions of mafic lavas which are low in K_2O and Rb content; the mafic late stage rocks of Mount Shasta are interpreted to be tholeiitic in composition. Mount Jefferson late stage volcanic activity (andesites and dacites) is characterized by high K_2O and Rb contents. The evolution of these magmas probably involves a very complicated procedure of tapping many magma chambers which could be receiving fresh magma and are at different stages of fractionation. However, the compositions are generally consistant with the theory of partial melting of ecologite, peridotite or amphibolite in, or above, a subduction zone and later fractional crystallization in several magma chambers.

INTRODUCTION

The stratovolcanoes; Mount Shasta, Mount Jefferson and Mount Rainier, form part of the high Cascades in California, Oregon and Washington, respectively (fig. 1). The purpose of this study is to evaluate the geochemistry of the lava extruded by these volcanoes and relate these data in terms of compositional variations to the evolution of the volcanoes. The resulting chemical relationships will facilitate a better understanding of the origin and evolution of the magma.

Theories on the origin and evolution of the magma have become numerous in recent years with the introduction and development of new global tectonics. The high Cascade Range represents an ideal geologic setting for studying volcanic rocks which have their theoretical origin in the upper mantle caused by the underthrusting of the oceanic crust. Mount Shasta and Mount Rainier were selected for this study because they are the two most voluminous volcanoes in the high Cascades and therefore offer a great number of volcanic flows to sample. These two volcanoes are on opposite geographical ends of the Cascade Range with Mount Jefferson in the center. Mount Jefferson exhibits severe dissection by glaciation with numerous lava flows easily accessible for sampling. The general geology of all three volcanoes is known and this acted as a guide for systematic sampling.

A total of 313 flows were sampled: 71 from Mount Shasta, 85 from Mount Jefferson and 157 from Mount Rainier. 168 flow samples were analyzed for silica and potassium and 69 samples were examined petrographically and analyzed for titanium, aluminum, iron, magnesium, calcium, sodium, zinc, copper, nickel, rubidium, strontium and cobalt. The sampling of volcanic flows [illegible] most successfully accomplished on exposed ridges and cleavers of the volcanoes, therefore, eliminating any doubt as to the relative ages of the flows. Stratigraphic columns representing compositional variations were constructed from this type of sampling procedure. In areas where the flow stratigraphy was not well exposed, sampling was based on a geographic distribution.

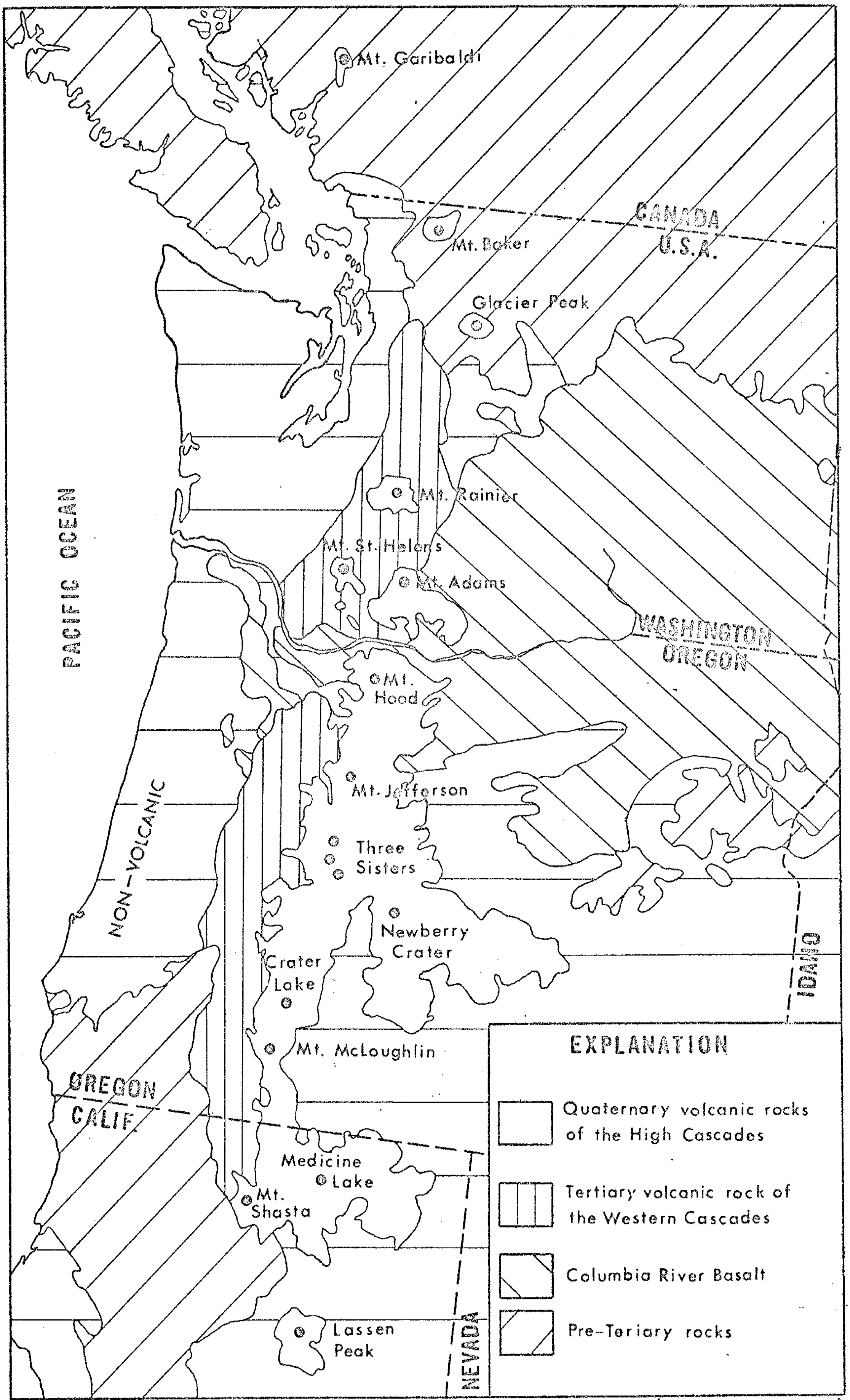

Figure 1. Generalized geologic map of the Cascades (McBirney, 1968).

SAMPLING

Sampling of the lava flows on Mount Shasta, Mount Jefferson and Mount Rainier was conducted in July and August of 1971. The purpose of the sampling program was to collect representative samples from volcanic flow sequences as well as from volcanic rock units exhibiting various age relationships and field distributions. Of course, a special attempt was made to avoid sampling weathered units.

Three separate samples, all from the same outcrop, were collected from each location. One sample was used for a thin section, another for chemical analyses and the third for a reference hand specimen which can be used for future work.

The sampling of flow sequences was best accomplished on ridges and cleavers of the various volcanoes. Good stratigraphic sections were sampled on Mount Rainier and Mount Jefferson but due to relatively poor outcrops, inaccessible outcrops or snow cover, stratigraphic relationships were not absolutely clear for Mount Shasta flows. However, representative samples were collected from the oldest lava, exposed in Mud Creek Canyon, to fresh young flows from satellite cone eruptions (fig. 2).

ANALYTICAL METHODS

Sample Preparation

The selection of rock samples to be chemically analyzed was based on; sample locations in flow sequences, age relationships of flows, field distribution and lack of weathering. Samples were checked both in hand specimen and in thin section for any weathering effects. All weathered surfaces, if present, were removed during the mechanical breakdown of the rock. The analyses were done by X-ray flourescence and pellets were made for this purpose. Sample preparation and X-ray analysis were conducted according to a procedure recommended by Dr. Condie.

The initial mechanical breakdown was done with a steel hammer and plate. The resulting sample size averaged 1/8" to 1/4" in diameter. Finer crushing was done in a small portable jaw crusher where particle size was reduced to under 1/8". The next crushing step was done on a porcelain buckboard. Here, particle size was reduced to 2 mm in diameter or less. The final crushing, finer than .085 mm, was done on an automatic Fisher Mortar Grinder.

The equipment used for grinding was constantly cleaned. All grinding tools and machines were cleaned twice and precontaminated before another sample was prepared. After the jaw crusher step, only one-quarter of the sample was reduced to powder.

The fine rock powder was then mixed with bakelite in a ratio of 6:1 making a total weight of 7±.0005 grams, which was weighed on a Mettler balance. Bakelite helped to make the pellets more durable, therefore, minimizing crumbling and breaking. The sample and bakelite mixture were homogenized with an automatic Spex Mixer with the aid of a plastic ball enclosed in the container. Each seven gram, 1 1/4" pellet was made in a steel die which was subjected to ten tons of pressure and about 300°C.

Analysis

All samples were analyzed by non-destructive X-ray flourescence using U.S.G.S. standards; W-1, AGV-1, T-1, GSP-1, GA, G-2 and BCR-1 to construct major element calibration curves. AGV-1 was used as the standard for all trace element analyses. The standard concentrations used are listed in Table 1a.

A linear electronic drift in the analyzing unit was not assumed and corrections for time fluctuations were made by normalizing a standard pellet, used as a drift pellet, to a standard number of counts. The remaining samples in a run were corrected by the ratio generated from normalizing procedures. Each sample was analyzed ten times per element and the mean value is recorded in this paper.

Other variables were also taken into consideration during analyses. These variables were: pellet homogeneity, sample holder position and alignment, minimum counts, duration of counting, peak to background ratios and operator error. Mr. Murray (August 1, 1971) determined that if these variables were optimized, which they were, and considering the fore mentioned method of sample preparation and analysis, an error of plus or minus three percent could be expected.

Exactly 168 samples of lava from all three volcanoes were analyzed for both SiO_2 and K_2O. 69 of these samples were selected for further analyses of Al_2O_3, TiO_2, Fe_2O_3, MgO, CaO, Na_2O, Zn, Cu, Ni, Rb, Sr and Co.

Table 1a. U.S.G.S. Standard Concentrations

	SiO_2	TiO_2	Al_2O_3	Fe_2O_3	MgO	CaO	Na_2O	K_2O	Zn	Cu	Ni	Co	Sr	Rb
W-1	52.64	1.07	14.85	11.09	6.62	10.96	2.15	.64						
AGU-1	58.88		17.01	6.80	2.04	4.98	4.33	2.89	83	63	20	17.5	665	68
T-1	62.65							1.23						
GSP-1	67.27	.69	15.11	4.33	2.30	2.03	2.88	5.48						
GA	69.90							4.03						
G-2		.53		2.76	1.44	1.98	4.15							
BCR-1		2.23	13.65	13.50		6.95	3.31							

Element oxides are expressed in weight percent.

Trace elements are expressed in ppm.

Precision and Accuracy

Precision is defined as the reproducibility of the results. The important components which contribute to the precision of chemical analyses are counting error, pellet reproducibility, electronic drift (short and long term) and pellet homogeneity.

Collection of X-ray pulses exhibit a normal or Gaussian distribution so the standard deviation (counting error) is:

$$\sigma = \sqrt{N}$$

N is the number of counts. The relative counting error (coefficient of variation) is:

$$\sigma\,\% = 100\sqrt{N}/N.$$

For analyses requiring background counts (when peak counts are less than an order of magnitude of the background counts) another equation is used:

$$\sigma = \sqrt{(Np + Nb)}.$$

Np is the total counts recorded under the peak and Nb is the number of counts representing the background. The relative counting error is:

$$\sigma\,\% = \frac{100\sqrt{Np + Nb}}{Np - Nb}$$

An overall expression for precision would be the square root of the summation of all the precision error squared.

$$\sigma = \sqrt{(\sigma_1)^2 + (\sigma_2)^2 + (\sigma_3)^2 + \text{etc.}}$$

Accuracy is defined as the correctness of the data. The largest contributing error is the accuracy of the standard which, of course, is related to the variation of previously reported concentrations of the standard. Average precision and accuracy values for the chemical analyses are reported in Table 1b along with the average relative counting error (σ %). The larger precision and accuracy values originate from a high background to peak ratio during counting.

Point Counting (Modal Analysis)

Point counting (using an electrical point counter) of 28 thin sections was conducted to determine mineralogical composition in volume percent. The first slide was counted so that the volume of each component was plotted every 200 counts up to a total of 3000 counts. This established the minimum number of points required for an accurate modal analysis. Fluctuations of the modal analysis were severe in the first several 200 count intervals but decreased with increasing point counts until an essentially constant volume was recorded above 1800 counts. The remainder of the point counting was done at 2000 points to insure accuracy. A grid of 0.3 mm by 1 mm was used so that the whole thin section could be covered.

Table 1b. Statistical Evaluation

	σ(%)	Overall Precision (%)	Overall Precision and Accuracy (%)*
SiO_2	1.0	3.2	$\leqslant$ 5.9
TiO_2	1.0	3.3	$\leqslant$ 5.9
Al_2O_3	0.8	3.1	$\leqslant$5.9
Fe_2O_3	0.2	3.0	$\leqslant$5.8
MgO	3.0	4.2	$\leqslant$6.6
CaO	0.2	3.0	$\leqslant$5.8
Na_2O	7.0	7.6	$\leqslant$9.1
K_2O	0.6	3.0	$\leqslant$5.9
Zn	17	17.5	$\leqslant$ 18.2
Cu	10	10.9	$\leqslant$11.9
Ni	21	21.4	$\leqslant$ 22.0
Co	23	23.4	$\leqslant$ 23.9
Rb	7.0	8.2	$\leqslant$ 9.6
Sr	0.8	4.3	$\leqslant$6.6

σ % = Counting error percent

$$\text{Overall Precision} = \sqrt{(\text{counting error})^2 + (\text{pellet reproducibility})^2 + (\text{electronic drift})^2 + (\text{pellet homogeneity})^2}$$

$$\text{Overall Precision and Accuracy} = \sqrt{(\text{overall precision})^2 + (\text{error of standards})^2}$$

*Assuming an error of 5% for the standards

GENERAL GEOLOGY

General Description

The high Cascades were formed during the Late Cenozoic (Callaghan, 1933). The volcanic rocks were primarily lava flows with interbedded volcanic ash beds, mudflow deposits and sedimentary rocks composed mostly of angular volcanic debris. The lava flows are considered to be calc-alkaline in nature. The rocks fall into the compositional range of andesite although the full gambit of volcanic rocks, that is, from iron-rich basalt to light colored silicic dacite and rhyolite, is represented.

As a general history of the evolution of the Cascades, several major episodes have been denoted below (McKee, 1972):

1. Deposition between late Eocene and early Miocene time of sedimentary and volcanic strata to a total thickness of 3 to 6 miles.
2. Folding, faulting and some intrusion of batholiths and stocks in the middle of the Miocene Epoch. Mountains produced by this orogeny were largely leveled by later Miocene erosion.
3. Partial burial of the range beneath lava flows of the Columbia River Basalt.
4. Late Tertiary volcanism and initiation of range uplifts.
5. Quaternary formation of the Cascade volcanoes during the continued uplift of the range.

In lower Tertiary strata, two distinct series have been recognized. The oldest series is generally late Eocene in age, and is composed of conglomerates, sandstones and siltstones interbedded with volcanic rocks. These rocks have been severely folded and show slight metamorphic alteration. The younger series rests unconformably on the Eocene rocks. In Oregon it is called the Little Butte Volcanic Series (western Cascades) and in Washington it is known as the Keechelus Volcanic Group. The age is considered to be Oligocene to perhaps early Miocene. It is interesting to note that the rock morphologies of the second series are very similar to volcanic sequences found in the Basin and Range Province. These rocks mostly include units of light colored volcanic ash (tuffs), massive flows of andesite and extensive layers of andesitic breccia. Basalt and dacite flows are commonly found together.

The modern Cascade Range is built on a Late Cenozoic uplift. The uplift is referred to as the Cascade uplift. The once horizontal flows of the Columbia River Basalt in northern Oregon and Washington have been arched extensively. The arch dictates a minimum uplift of 2800 feet since Miocene time in this section of the Cascades. However, due to the lack of exposed thick, stratigraphic sections, the uplift is questionable for the Cascade Range south of Bend, Oregon. Much of the southern part of the Cascade Range owes its base elevation to the accumulation of the late Tertiary lava and pyroclastic debris rather than uplift (McKee, 1972).

Cascadian andesitic volcanism may have started in the Pliocene and most of the cones have been victims of erosion but plugs still remain. The impressive volcanoes of the Cascade Range today were definitely formed in the Quaternary Period. In fact, the entire sequence of rocks at Mount Jefferson, the Three Sisters and possibly Mount Mazama appears to be normally polarized so they can be considered younger than the last magnetic reversal 770,000 years ago (McBirney, 1968). The young volcanoes of the Cascade Range form part of the North American link in a nearly continuous circum-Pacific ring of volcanoes. Their Quaternary histories are thought to be similar to most other circum-Pacific volcanoes including the Aleutians, Kamchatka, Japan, the Andes and the southwest Pacific island volcanoes. Calc-alkaline volcanic rocks are numerous in most of these areas. The major difference being that the Andes and the Cascades are noticeably higher in alkalies ("continental type" volcanoes) with respect to the island arc volcanoes in the Pacific.

GENERAL GEOCHEMISTRY

Cascade Geochemistry To Date

Some earlier studies of the Cascade volcanoes proved to be more than a reconnaissance. These were done by Howel Williams at Crater Lake (1942) and Lassen Peak (1932) and T. P. Thayer at Mount Jefferson (1937). In addition, R. S. Fiske and others at Mount Rainier (1963), W. S. Wise at Mount Hood (1969), R. C. Greene in the Mount Jefferson area (1968) and Smith and Carmichael in the Southern Cascades (1968) have contributed significant geochemical data.

Existing geochemical data suggests that the volcanoes are one of two types. In the first type, a coherent series of lavas are very uniform in composition and exhibit a limited chemical range of continuous variation. In the second type, the lavas show a varied chemical range which becomes even more divergent with time (McBirney, 1968).

The chemical data available in the literature indicates that the lavas of the high Cascades are compositionally within the range of the calc-alkaline series (Jakes and White, 1972). This series includes hi-alumina basalt, andesite, dacite and rhyolite. The calc-alkaline series is chemically distinguishable from other volcanic series primarily on the basis of major-element chemistry, particularly K_2O versus SiO_2, total alkalies versus SiO_2, the K_2O/Na_2O ratios and iron enrichment in AMF diagrams. Trace element geochemistry similarly exhibits definitive volcanic trends. These relationships have been pointed out by Ewart et al. (1968), Gorshkov (1969), Gill (1970), Hart (1970), Jakes and Gill (1970), Jakes and White (1970, 1972), Lowder and Carmichael (1970), Pushkar (1968), Shaw (1968), Siegers et al.

(1969), Taylor and White (1966), Taylor et al. (1969a) and Taylor et al. (1969b).

The geochemistry of Cascade volcanic flows represents an intermediate stage in island arc or continental margin growth. Primary volcanic growth results in lava of the tholeiite series which is exemplified in the early stages of island-arc development. The mature stage is equivalent to the Andean lava of the shoshonite series or late stage island-arc development. Calc-alkaline volcanism is presently thought to represent the intermediate stage of growth (Jakes and White, 1972).

Many chemical classifications of volcanic rocks have been set forth in literature. This paper will follow the classification of the calc-alkaline series (Table 2) used by Taylor (1969) and volcanic series definitions of Jakes and White (1972).

Formation Theory of Coherent and Divergent Volcanoes

Most of the volcanoes of the north central Cascades; Baker, Rainier, Hood and Jefferson, tend to produce coherent lava, that is, lava that shows a continuous chemical trend. The volcanoes on the north and south ends of the Cascade Range exhibit lava of the divergent type (McBirney, 1968). There are, of course, exceptions to this observation. It is interesting that the central region of the Cascade Range was formed on an embayment between areas of pre-Tertiary sialic basement rock which outcrops in the northern and southern end of the range (fig. 1). The first theory suggests that the embayment contributes to the chemical continuity of the magma producing mechanism. This fact may be coincidental or incomplete sampling of the volcanoes could be responsible for McBirney's geochemical observation. McBirney's evidence for coherent and divergent lava stems from AMF diagram observations of existing data. AMF diagrams (fig. 24) resulting from this study would suggest all three volcanoes to be of the coherent type.

An alternative theory involves the close association of the Miocene epizonal plutons to the central Cascade volcanoes. It has been suggested (Hopson et al., 1965) that the source of the coherent lavas was from plutons that remained active at depth. The plutons intersect the Cascade volcanic chain in the same proximity as the coherent volcanoes are found. Again the lack of complete sampling, therefore a limited number of chemical analyses, could indeed suggest such a theory.

Table 2. Calc-alkaline Series Classification

High-Al basalt: 53% SiO_2

Low-Silica andesite: 53-56% SiO_2; 0.7-2.5% K_2O

Low-K andesite: 0.7% K_2O 53-62% SiO_2

ANDESITE: 56-62% SiO_2; 0.7-2.5% SiO_2

High-K andesite: 2.5% K_2O; 53-62% SiO_2

Dacite: 62-68% SiO_2

Rhyolite: 68% SiO_2

MOUNT SHASTA

Geologic Setting

With the exception of Lassen Peak, Mount Shasta is the most southerly of the Cascade Range volcanoes. Mount Shasta has grown 10,000 feet in elevation above its base to an elevation of 14,161 feet. The parasitic cone, Shastina, has reached an elevation of over 12,000 feet. The volcano has an average diameter of 17 miles and has produced 80 cubic miles of lava (Williams , 1934). This volume of lava exceeds any other calculated volume produced by a Cascade volcano. The initial growth of the volcano probably started in the Pleistocene and volcanism continued to a few hundred years ago.

Glaciers were responsible for most of the erosion on Mount Shasta. Five active glaciers remain although they are rapidly receding. Hot spring activity continues near the summit of the mountain.

H. Williams (1934) suggests that Mount Shasta overlies or is associated with an alkali-olivine basalt which was probably erupted from a shield volcano. These rocks outcrop to the south of Mount Shasta (fig. 2).

History of Development

Relative age relationships of the volcanic rocks in the Mount Shasta area are not well known due to the complexity and diversity of the volcanic features. Only educated guesses can be made from Howel Williams' work (1934), personal field work and air-photo studies. Nevertheless, these observations suggest three major periods of volcanic activity.

Figure 2. A general geologic map of Mount Shasta area, California, showing sample locations. Geology after Williams (1932b; 1934).

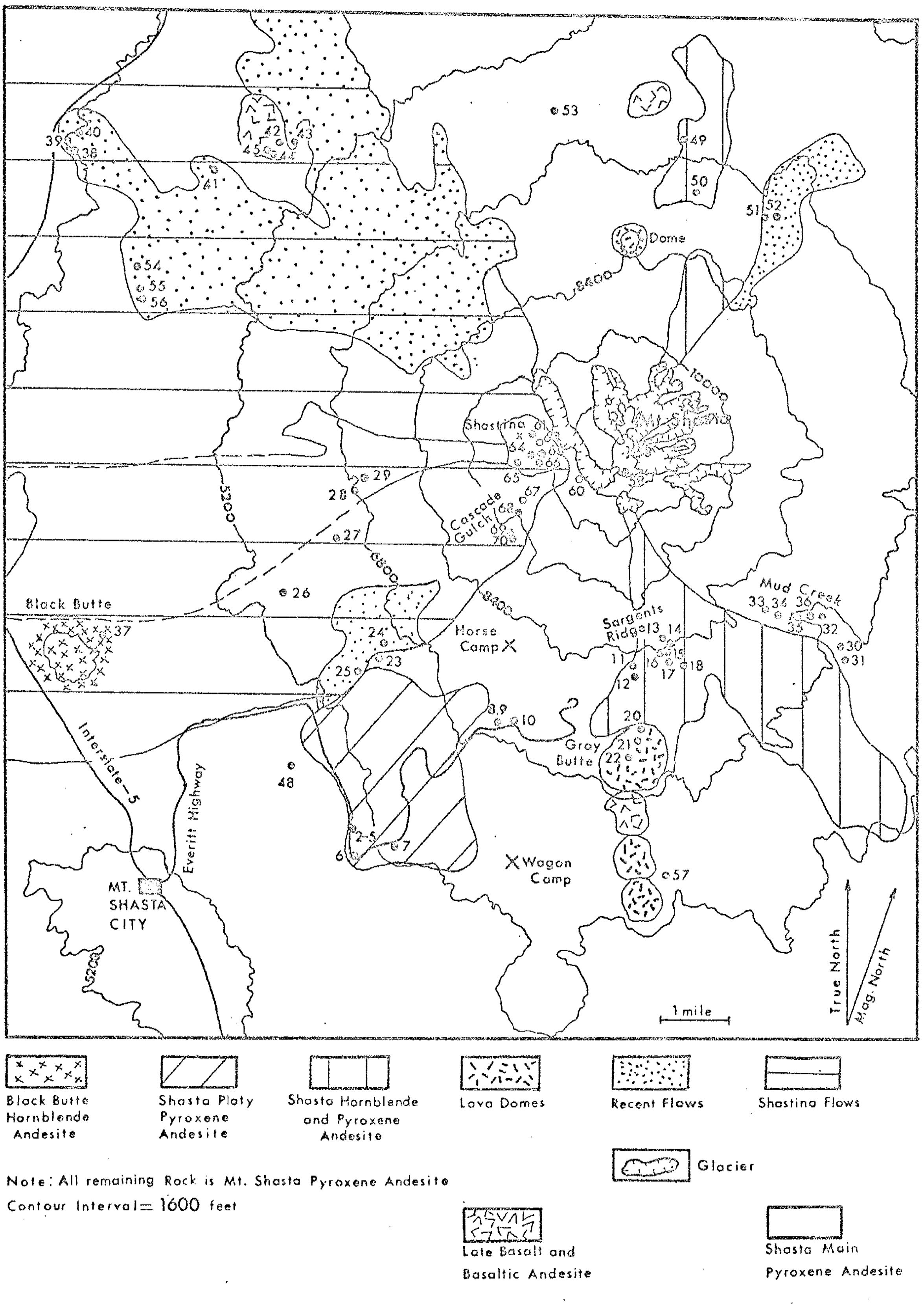

The earliest Quaternary volcanic activity in the area started with the growth of Mount Shasta proper. In general, these rocks are uniform pyroxene andesites and dacites that are similar in texture. The growth of Shasta volcano ceased with an andesite dome forming in the main vent.

The second period of volcanism is characterized by the formation of andesite domes and two basaltic cinder cones along a north-south axis. Williams (1934) relates the location of these features to a north-south trending fissure. The fissure developed late in the volcano's history and may have been responsible for the implacement of the summit dome on Mount Shasta.

The third and final major period is represented by the formation of the large parasitic cone, Shastina, on the west side of Mount Shasta. Black Butte and young flows on the lower flanks of the volcano also formed in this period (fig. 2). These features are thought, by Williams (1934), to be related to an east-west fissure which formed some time after the north-south fissure. Shastina and Black Butte lava is essentially hornblende dacite and the young flows are pyroxene andesites and dacites. Minor flows of a younger age have erupted from small satellite cones at low elevations and are basalts and basaltic andesites in composition.

Petrology

The dominant lava of Mount Shasta is pyroxene andesite in which hypersthene usually exceeds augite. Hypersthene phenocrysts (determined by Hull-Debye-Sherrer powder method) tend to group together with augite to form glomeroporphritic clots. Albite-twinned plagioclase and opaques fill interstitial spaces. Olivine and mica were reported as rare (Williams, 1934), however, not a trace of either mineral was found in the present study; orthopyroxene replaces olivine as fractional crystallization progresses.

Two generations of plagioclase crystals exist in these rocks. The larger plagioclase phenocrysts have reaction rims and are oscillatory zoned with a compositional range from An_{50} to An_{60}. Their rounded shapes suggest resorption and some have clinopyroxene inclusions. The younger plagioclase phenocrysts are sharply defined and exhibit prominent albite twinning with a compositional range from An_{22} to An_{30} (Michael-Levy Method). Modal analyses of some of the flows in sequence are represented in Table 3. In hand specimen these rocks are various shades of gray with readily visible plagioclase and pyroxene phenocrysts. The texture of the groundmass is fine and rarely develops into a coarse texture; most flows are strongly prophyritic.

Hornblende rarely occurs in Mount Shasta flows (approximately 5%) but is associated with Shastina volcanism. The rare occurrence of hornblende in Mount Shasta flows probably results from extensive reaction with the magma and the thick reaction rims produced usually consist of opaque minerals. In the Black Butte dome (hornblende dacite) hornblende, up to an inch long, comprises as much as 20 percent of the phenocrysts; pyroxene is not present and the remaining phenocrysts are plagioclase. The hornblende has been partially replaced by magnetite and, to a lesser degree, hematite.

Glass in the groundmass is uncommon in most of the rocks examined. However, black and brown glass occasionally constitutes

MT. SHASTA

	Sargents Ridge					Mud Creek			Cascade Gulch			
	18	17	15	14	13	31	30	34	60	68	69	70
Plagioclase (large)	17.1	18.9	12.3	23.3	25.0	10.0	17.8	17.7	1.6	---	17.5	4.8
Plagioclase (small)	12.9	15.4	26.5	11.6	12.2	36.9	22.8	11.4	37.4	29.1	7.2	22.1
*Groundmass	59.0	56.4	56.1	58.2	55.7	47.3	52.8	63.0	57.6	68.3	69.8	66.6
Clinopyroxene	5.3	4.1	2.1	1.1	1.3	3.3	2.2	3.1	1.7	.7	2.3	4.6
Orthopyroxene	4.9	4.2	2.9	4.2	4.8	2.5	3.4	2.7	1.2	.6	2.8	1.2
Opaques	.8	1.0	.1	1.6	1.0	---	1.0	2.1	.5	.8	.4	.7
Hornblende										.5		
Total	100.0	100.0	100.0	100.0	100.0	100.0	100.0	100.0	100.0	100.0	100.0	100.0

*Groundmass also includes glass and voids.

Table 3. Mt. Shasta Modal Analysis (volume percent).

up to 20 percent of some flows and Williams (1932b, 1934) reports glass contents up to 40 percent in some of the early Mount Shasta flows. Glass is occasionally stained with iron oxides, usually magnetite.

Mafic inclusions can be found in Mount Shasta flows. Mineralogically they appear to be a low-silica andesite with resorbed hornblende. The inclusions probably represent remnants of an earlier flow or early crystallization in a magma chamber which fed Mount Shasta volcanism.

Geochemistry

The lavas studied vary chemically from hi-alumina basalt in very recent flows associated with Shastina to dacite related to Shasta and Shastina development. The geochemical distribution in the andesites and dacites indicates that Mount Shasta is basically a calc-alkaline volcano. The Shastina flows have very low K_2O contents, similar to tholeiitic volcanic rocks from Viti Levu, Fiji (Gill, 1970) and St. Kitts (Baker, 1968). Both Shasta and Shastina rocks are plotted on Kuno's (1966, 1969) SiO_2-alkali variation diagram (fig. 22) and most of the points fall in an area described as being derived from tholeiitic basalt. Most of the lava from Shasta is andesitic or dacitic in composition and varies in SiO_2 from 60 to 68 percent. Smith and Carmichael (1968) have pointed out that Shastina andesites are tholeiitic and relatively rich in calcium and magnesium; these concentrations are similar to Shasta andesites and dacites (figs. 9 and 10). The higher concentrations of calcium and magnesium reflect the relatively high modal volume of the pyroxenes. Magnesium, sodium, aluminum and calcium distributions in Mount Shasta flows closely compare with other calc-alkaline chemistry (Taylor and White, 1966; Taylor et al., 1969; and Jakes and White, 1972). Titanium increases as Fe_2O_3 increases and a constant TiO_2/Fe_2O_3 ratio of 0.125 is maintained. Total iron is reported in this paper as Fe_2O_3. The alkali-magnesium-iron relationship exhibits lower iron concentrations than tholeiitic trends. Consequently, Mount Shasta points on the AMF diagram (fig. 24) indicate a calc-alkaline trend.

The rubidium SiO_2 variation diagram reveals considerable scatter of points (fig. 12). However, these concentrations are consistent with other calc-alkaline volcanic rocks found in New Zealand (Ewart et al., 1968) and Talasea (Lowder and Carmichael, 1970). Rubidium as well as strontium, zinc, copper and nickel (figs. 11 and 12) do not indicate chemical variation related to rock types of the Shasta area.

Nickel, zinc and copper variation diagrams show considerable point scattering but their concentrations remain relatively constant within a range as SiO_2 increases (fig. 11). The average concentration is about 15 ppm for Ni, 50 ppm for Cu and 80 for Zn. Cobalt also exhibits a constant relationship with SiO_2 concentrations but at a slightly lower value of about 10 ppm (fig. 12). Zinc and copper are the only two trace elements which show a systematic variation with each other (fig. 23). The zinc relationship is bimodal and copper varies in concentration with respect to the two average zinc concentrations of 75 ppm and 95 ppm.

The potassium-rubidium ratio is low for calc-alkaline andesite (based on Shaw, 1968) and due to the scatter of the strontium data, potassium-strontium ratios are erratic (Table 6). The calcium-strontium ratios (Table 6), in general, decrease with fractionation indicating more strontium is admitted into the calcium lattice site in plagioclase as silica increases (and fractionation continues). All Mount Shasta chemical analyses are represented in Table 6.

MOUNT JEFFERSON

Geologic Setting

Glacial erosion has highly dissected Mount Jefferson to expose as much as 7,500 feet of relief. The elevation is 10,493 feet and Mount Jefferson is in the high Cascade Range which, in this area, is only a north-south trending ridge. The crest of the ridge varies in elevation from 5,500 to 6,500 feet. Deep U-shaped valleys terminate at steep headwalls against the west side of the ridge (fig. 3).

The first work on Mount Jefferson geology was reported by Hodge (1925) and he briefly discussed the volcanic rocks, glacial history and general physiography. Thayer (1937) described the petrology of the rocks and distinguished the lava of the Mount Jefferson area (high Cascades) from those of the Western Cascades. Thayer, from sixteen chemical analyses, concluded that Mount Jefferson rocks were poor in K_2O and total iron but richer in Al_2O_3 than the rocks of the Western Cascades. Thayer later (1939) described additional structural details of the Mount Jefferson flows.

Underlying the Mount Jefferson area are sedimentary rocks which can be correlated with those of the Miocene and Pliocene rocks of the Western Cascades (Peck et al., 1964). Lava flows with cinder units and breccia are also found beneath the area (Callaghan, 1933; Peck et al., 1964); they are Pliocene to Recent in age, undeformed and range from basalt to rhyodacite in composition. Recently, the general geology of the Mount Jefferson Primitive Area has been described by Walker et al. (1966) and the petrology and some geochemistry was reported by Greene (1968).

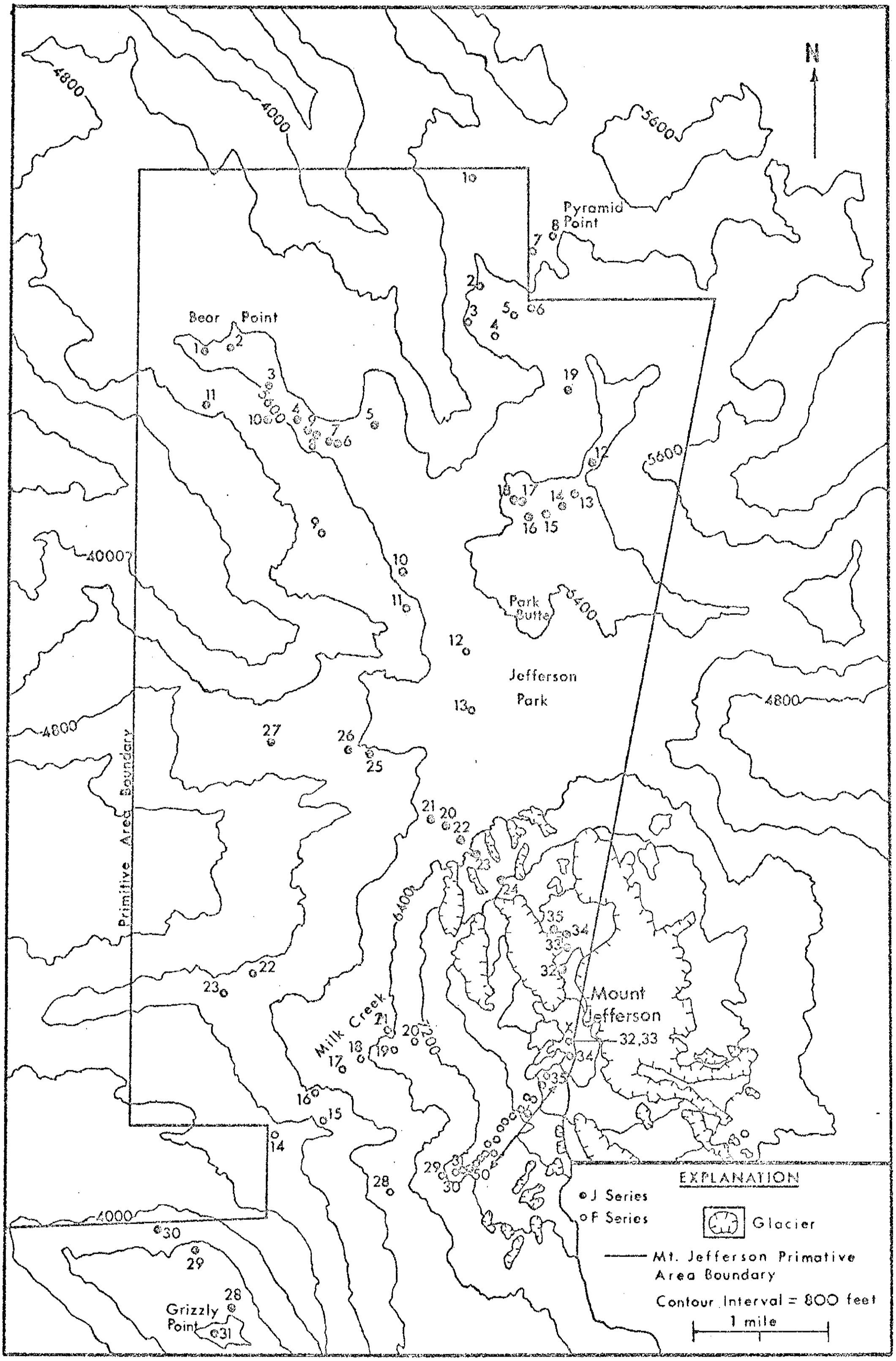

Figure 3. Sample location map of Mount Jefferson, Oregon. Essentially the whole area is composed of andesite flows with few exceptions. Geology after Walker et al. (1966).

Mount Jefferson is a dissected stratovolcano with a predominant rock type of pyroxene andesite and some pyroxene dacite. The andesite flows range in thickness from about one foot to about 10 feet. These flows, frequently interbedded with pyroclastics, are usually a shade gray and commonly exhibit cooling joints.

Petrology

The porphyritic volcanic flows of Mount Jefferson are similar in mineralogy. The phenocrysts are plagioclase (26-40%), clinopyroxene (1-6%), orthopyroxene (1-6%) and opaque Fe-Ti oxides (.5-3%). In the andesites, plagioclase exhibits two periods of generation as did the plagioclase from Mount Shasta. The large plagioclase composition is labradorite to bytownite; the smaller plagioclase phenocrysts have a lower and widely variable An content. The larger plagioclase phenocrysts are oscillatory zoned and show resorption around the edges of the crystals. The smaller plagioclase crystals are fresh looking and show sharp contrasts with the groundmass.

Although olivine has been reported in the andesites (Green, 1968), only traces were found in this study. All of the rocks examined petrographically had orthopyroxene and if olivine did form an early crystallization phase it probably has been removed by reacting with the magma. Clinopyroxene (augite) dominates over the orthopyroxene (hypersthene) in about half of the thin sections examined (see Table 4 for modal analyses). Pyroxene frequently fills interstitial spaces in the plagioclase phenocryst groups.

Opaques are usually anhedral magnetite grains although opaque iron oxide stains are common. Glass is present in most of the flows

MT. JEFFERSON

Southwest Summit

	F29	F49	F46	F42	F39	F37	F35	F32
Plagioclase (large)	16.6		7.7	6.4	7.6	9.6	8.7	20.2
Plagioclase (small)	13.9	31.2	24.8	24.4	25.0	16.5	23.0	14.6
*Groundmass	60.1	66.9	58.8	63.4	59.3	62.8	59.1	54.1
Clinopyroxene	3.6	1.1	3.6	1.2	1.1	3.0	2.6	5.5
Orthopyroxene	3.4	.8	3.1	4.3	6.1	5.1	4.8	3.0
Opaque	2.4		2.0	.3	.9	3.0	1.8	2.6
Total	100.0	100.0	100.0	100.0	100.0	100.0	100.0	100.0

*Groundmass also includes glass and voids.

Table 4. Mt. Jefferson Modal Analysis (volume percent).

and can constitute up to 25 percent of the groundmass. The glass is usually brown but occasionally black.

In the silicic andesites, olivine is not present and the larger plagioclase phenocrysts are less abundant than the small plagioclase phenocrysts. The predominant pyroxenes are again augite and hypersthene. Very minor amounts of hornblende are present but generally they have been replaced by opaque minerals. The groundmass is very fine and the flows are vesicular. The dacites sampled have mineral assemblages comparable to the silicic andesites.

Geochemistry

The sampling of Mount Jefferson was accomplished by making two traverses from the base of the volcano to summit plug. Sampling traverses were made along the Northwest Ridge and Southwest Ridge (fig. 3) where readily accessible stratigraphic sections occur. Low elevation samples were collected from the Milk Creek area. Lava flows related to Mount Jefferson were also sampled at Grizzly Point, Jefferson Park, Bear Point and Pyramid Point.

Potassium data indicates that these flows are similar to known calc-alkaline volcanics from Viti Levu, Fiji (Gill, 1970) and Akagi, Asama, Iwaki, Japan (Kuno, 1962). However, with respect to the low K_2O and Rb concentrations, these flows appear to be transitional between calc-alkaline and arc-tholeiite series as defined by Jakes and White (1972). Also, a $K_2O + Na_2O$ versus SiO_2 diagram (fig. 22) shows the Mount Jefferson points in an area defined by Kuno (1966, 1969) to represent a parental material of hi-alumina basalt which is part of the calc-alkaline series.

TiO_2, Fe_2O_3, MgO and CaO appear to decrease as SiO_2 increases (figs. 13 and 14). K_2O and Na_2O values increase slightly with increasing SiO_2 (figs. 14 and 22) and the scattered Al_2O_3 concentration remains constant within a range of 16 to 18 percent as SiO_2 increases (fig. 14). The major element geochemistry is compatable with known major element geochemistry of calc-alkaline volcanics (Jakes and Smith, 1970; Jakes and White, 1970; and Jakes and White, 1972).

Co, Rb, Sr and Zn concentrations remain almost constant within narrow ranges when compared on SiO_2 variation diagrams (figs. 15 and 16). The scattered Cu and Ni concentrations appear to decrease slightly as SiO_2 increases. All trace element concentrations are comparable to other calc-alkaline rock concentrations (Taylor and White, 1966; Ewart et al., 1968; Ewart and Stipp, 1968; and Taylor et al., 1969b) with the exception of Rb which has concentrations similar to arc-tholeiites which are found on Viti Levu, Fiji (Gill, 1970) and as described by Jakes and White (1972).

Chemical variation is compared to stratigraphic height in figures 4 and 5 for the Southwest section. This section represents approximately 1,000 meters in thickness. The chemical variations, in general, are not systematic, that is, the variations of the major and trace elements (figs. 4 and 5) do not behave in a manner which can be predicted by theories of fractional crystallization or partial melting. A more complex process of magma development must be involved to produce the irregular chemical evolution of lava flows. However, two chemical unconformities are present in the stratigraphic column between flow numbers 37 and 39, and 47 and 48. The chemical variations are minimal in each of the three sub-sequences and abrupt changes occur in some of the elemental distributions at the unconformities. Modal analyses of eight of these flows (Table 4) do not either indicate these unconformities or any mineralogic development within a sub-sequence. Chemical analyses for Mount Jefferson are listed in Table 7.

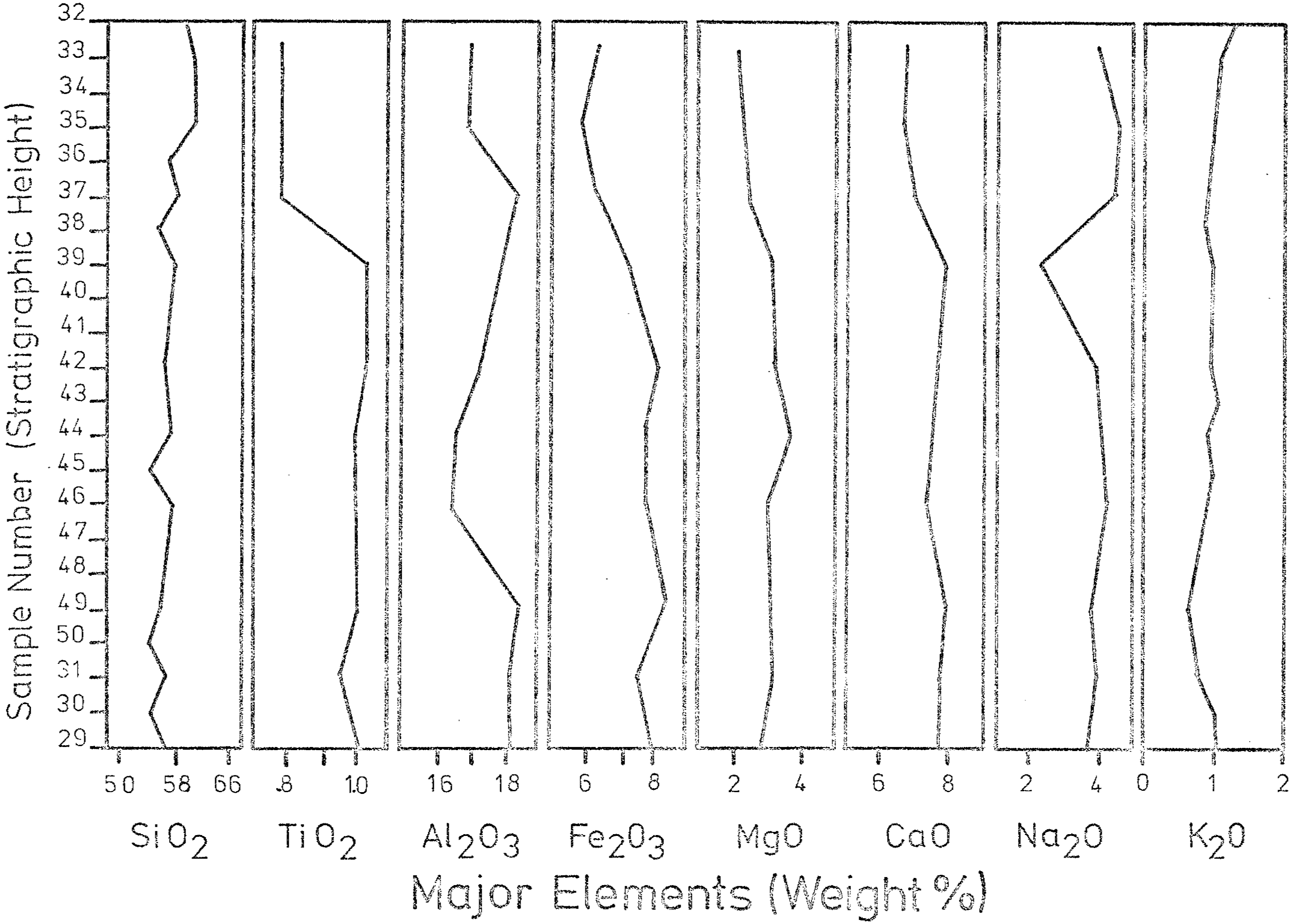

Figure 4. The stratigraphy of Southwest Summit Ridge, Mount Jefferson, compared to major element compositional variations. Flow stratigraphy is represented by arbitrary vertical units.

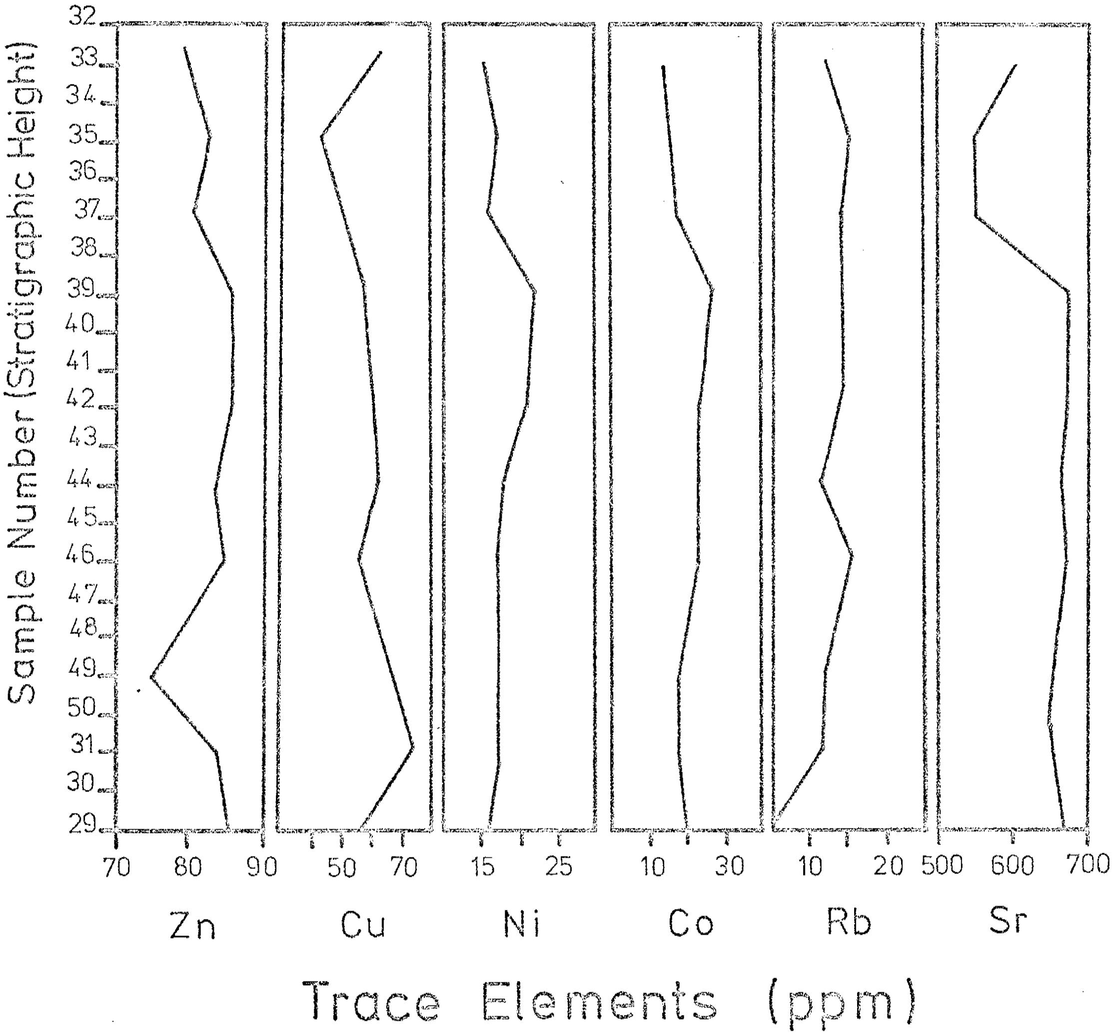

Figure 5. The stratigraphy of Southwest Summit Ridge, Mount Jefferson, compared to trace element compositional variations. Flow stratigraphy is represented by arbitrary vertical units. Samples from flow units having a full chemical analysis are 29, 31, 33, 35, 37, 39, 42, 44, 46 and 49; those with only SiO_2 and K_2O for concentrations are 30, 32, 36, 38, 43, 45 and 50; those without chemical analyses are 34, 40, 41, 47 and 48.

MOUNT RAINIER

Geologic Setting

Mount Rainier is a stratovolcano attaining an elevation of 14,410 feet. It is the highest volcano in the Cascade Range and is the second most voluminous (Williams, 1934). Mount Rainier National Park is 378 square miles in size and the total relief in the park is 12,850 feet. The relief of Mount Rainier flows is 7,000 to 8,000 feet. The rugged terrain presents quite a challenge for sampling with the best sections for sampling usually occurring at higher elevations along cleavers. These slopes are frequented by avalanches and are bordered by glaciers with deep crevasses. Unfortunately, sampling was difficult below about 5,000 feet because much of the park is covered with dense vegetation. This study of Mount Rainier covers the Mount Rainier flows only and no attention was given to the lower and middle Tertiary rocks in the area.

Mount Rainier is chiefly composed of pyroxene andesite flows although pyroxene dacite and olivine basaltic andesite flows are also present and were sampled (fig. 6). Mudflows, breccias and ash flows make up part of the composite cone but are relatively minor in volume. The volcano attained its height in the Pleistocene (Fiske et al., 1963) and glaciers have deeply eroded the mountain.

Mount Rainier is built mainly on the rocks of the Tatoosh pluton (grandiorite) and the Stevens Ridge Formation (rhyodacite ash flow). Thick intracanyon flows, like Rampart Ridge, are the earlier of the Mount Rainier flows. These early flows are not only large but many of them erupted in rapid succession (Fiske et al., 1963). These flows form the base of the volcano and the volcano probably grew

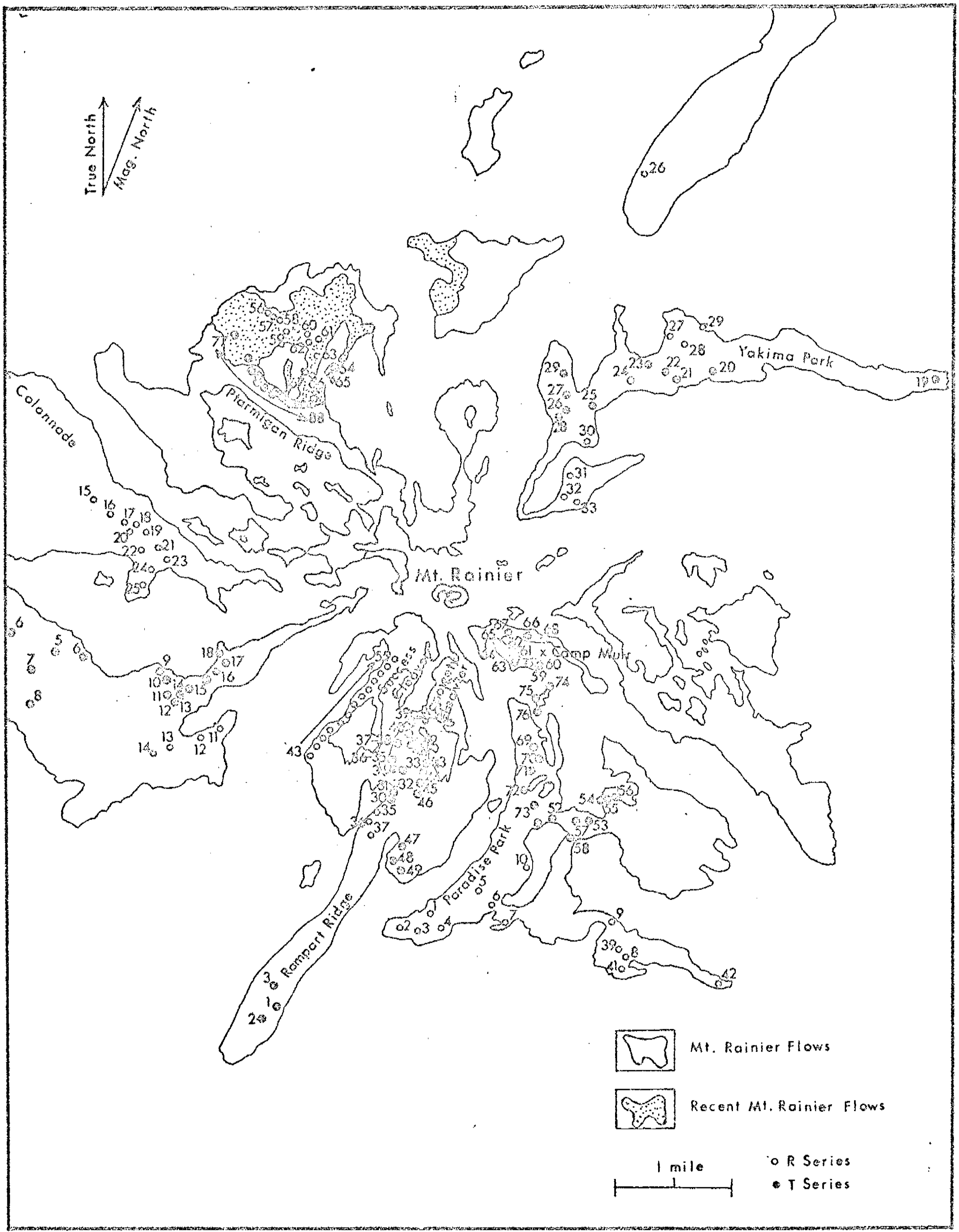

Figure 6. Mount Rainier, Washington, a generalized map showing the Mount Rainier lava flows. (Mount Rainier flows are pyroxene andesites and the recent flows are basaltic andesites.) Geology after Fiske et al. (1963).

rapidly in its early stages.

The main cone is composed of hundreds of thin lava flows, some interbedded with breccias and volcanic ash. The andesites are gray in hand specimen and the textures vary greatly depending on whether the rock cooled as a thin flow or as a pool near the base of the volcano. Most of the rocks are porphritic. Well developed columnar jointing occurs in the thicker flows and platy jointing in the thinner flows. Pale gray, radial dikes, which are vertical, occur at several locations.

Eruptions from Echo Rock and Observation Rock have been sampled. These two satellite cones erupted olivine basaltic andesite after Mount Rainier attained its present elevation. These flows are represented on figure 6 as Recent Mount Rainier flows and they erupted from the flanks of Mount Rainier about 550 years ago (Fiske et al., 1963).

Petrology

Hague and Idding (1883) first realized that the andesite erupted from Mount Rainier was uniform in composition. Almost all of the rocks observed were pyroxene andesite except for the Recent Mount Rainier flows which were called olivine andesite.

The pyroxene andesites are usually strongly porphritic. In most of the rocks observed there are two generations of plagioclase; lavas of Mount Shasta and Mount Jefferson exhibit this also. The larger plagioclase phenocrysts are strongly zoned while the smaller plagioclase crystals exhibit albite twinning and the crystal boundaries are very sharp. Occasionally, the larger plagioclase crystals clot together in a semi-parallel fashion to form glomerocrysts that are about An_{60} in composition. Both progressive and oscillatory zoning are evident in the plagioclase crystals. The same flow observed in several thin sections may vary considerably and is perhaps caused by turbulence and metastable crystallization in the magma chamber.

The pyroxene phenocrysts are smaller than either generation of plagioclase crystals except when they form in glomeroporphritic clots. Hypersthene (as determined by X-ray diffraction, Hull-Debye-Sherrer powder method) is the dominant orthopyroxene. It is present as 0.2 mm to 1 mm size phenocrysts and minute crystals are also found in the groundmass. Some of the hypersthene crystals exhibit reaction rims of opaque minerals while others have been partially replaced by augite (modal analyses on Table 5).

Augite is the dominant clinopyroxene and commonly occurs with hypersthene to form glomeroporphyritic clots. In about half of the flows it is subordinate to hypersthene. No pigeonite was observed.

Fiske et al. (1963) reports olivine in about half of the pyroxene andesite flows although it is rarely recorded in this study. The olivine appears to have extensively reacted with the coexisting magma to form opaques, hypersthene or augite. Olivine is readily seen in the Recent flows of Mount Rainier which are the olivine basaltic andesites. Hornblende sporatically occurs in only a few flows and usually appears unstable as it is thickly rimmed or completely replaced by opaques, usually magnetite. Hypersthene or augite occasionally form rims on hornblende phenocrysts.

Magnetite occurs in all flows. It is associated with plagioclase phenocrysts and is a slightly resorbed euhedral grain. Apatite occurs

MT. RAINIER

	Camp Muir				Wapowety Cleaver			
Samle	60	62	63	65	31	34	37	38
Plagioclase (large)	11.3	15.0	21.8	21.6	24.3	25.8	29.8	32.2
Plagioclase (small)	14.7	15.8	12.6	10.9				
*Groundmass	64.2	62.5	55.8	56.8	67.2	64.4	63.2	58.8
Clinopyroxene	5.9	1.8	5.4	5.8	4.4	4.6	2.9	4.0
Orthopyroxene	2.2	3.9	3.7	3.4	2.4	2.1	2.2	3.7
Opaque	1.7	1.0	.7	1.5	1.7	3.1	.9	1.3
Total	100.0	100.0	100.0	100.0	100.0	100.0	100.0	100.0

* Groundmass also includes glass and voids.

Table 5. Mt. Rainier Modal Analysis (volume percent).

as a very minor accessory mineral. No biotite is present in the flows.

Geochemistry

Mount Rainier's two general rock types, which are geographically distinct, are also chemically distinct. The pyroxene andesites and dacites have a SiO_2 content of 58 to 67 percent with K_2O concentrations above 1.5 percent, while the olivine basaltic andesite ranges from 55 to 58 percent SiO_2 and has K_2O concentrations below 1.5 percent (fig. 21). The K_2O concentrations are scattered but the K_2O-SiO_2 relationship is similar to calc-alkaline volcanics of Bougainville (Taylor et al., 1969a), Kirisima and Daisetu, Japan (Kuno, 1962, 1969), Klinchevskoi and Sheveluch, Kamchatka (Gorshkov, 1970) and Paricutin, Mexico (Mooser et al., 1958). In a $K_2O + Na_2O$ - SiO_2 variation diagram (fig. 22) a parental magma of hi-alumina basalt is indicated (after Kuno, 1966, 1969) which is part of the calc-alkaline series. Andesites and dacites, and basaltic andesites remain chemically distinct in all other major element - SiO_2 variation diagrams (figs. 17 and 18). Fe_2O_3 and CaO concentrations decrease as SiO_2 increases. TiO_2, Al_2O_3, MgO and Na_2O concentrations remain relatively constant in the SiO_2 range with the exception of the MgO content of basaltic andesite which sharply decreases in concentration as SiO_2 increases from 55 to 58 percent. The andesites and dacites have lower TiO_2, Fe_2O_3 CaO and MgO concentrations than the basaltic andesite and similar concentrations of Na_2O and Al_2O_3 (figs. 17 and 18).

Trace elements Zn, Cu, Ni, Co and Rb exhibit wide and scattered variations (figs. 19 and 20). Zn, Cu and Ni variation diagrams do not show a systematic relationship with SiO_2. Co and Rb data are scattered but the basaltic andesites form distinct groups relative to the andesites and dacites; Co is higher and Rb is lower in the basaltic andesites. Sr concentrations remain constant within the SiO_2 range (fig. 20). The zinc-copper variation diagram (fig. 23) reveals four or five chemical groupings of which the lowest concentration group is represented by basaltic andesite. Generally, very poor systematic relationships result when trace elements are compared to each other.

The Rb-SiO_2 relationship of Mount Rainier volcanics are similar to calc-alkaline volcanics of New Zealand (Ewart and Stipps, 1968) Northern Chili (Siegers et al., 1969) and Cape Nelson, Eastern Papua (Jakes and Smith, 1970). Sr concentration of the basaltic andesite is similar to the alumina basalts from Mount Lassen (Smith and Carmichael, 1968), however, in general, most of Mount Rainier trace element concentrations are similar to other calc-alkaline andesites (Jakes and Smith, 1970; Jakes and White, 1970, 1972).

Detailed sampling was completed on Success, Wapowety, Colonnade, Cowlitz, Cathedral Rocks and Lower Puyallup Cleavers. Paradise, Ptarmigan Ridge, Yakima Park, Camp Muir and Spray Park areas were also sampled. The stratigraphic sections presented in this paper are from Success Cleaver and Ptarmigan Ridge.

Major and trace elements for Success Cleaver lava flows (approximately 800 meters thick) are presented on a stratigraphic section exhibiting chemical variations (fig. 7). The major and trace element variations appear to be non-systematic with stratigraphic height although major element contents remain relatively uniform throughout the section. Trace elements Zn, Cu, Ni and Sr, however, exhibit considerable variation in the section. Major element data suggests a chemical unconformity between flows 52 and 53 (fig. 7), also SiO_2 and K_2O data imply another unconformity between flows 45 and 46. Even though trace element data agrees with the upper unconformity, it also suggests several others not exhibited by major element variation; no trace element data are available on the lower unconformity (between flows 45 and 46). Like the Southwest Ridge section of Mount Jefferson, three possible sub-sequences can be determined with unsystematic chemical variations in each.

The Ptarmigan Ridge section represents approximately 150 meters of young olivine basaltic andesite extruded from a satellite cone on the northwest flank of Mount Rainier. The geochemical data for six of these flows are compared to stratigraphic height on figure 8. The stratigraphic column suggests a gross systematic variation in many elements with respect to stratigraphic height. SiO_2 increases from 53 to 57 percent; Al_2O_3, Zn, Cu and Co also grossly increase in concentration in this section. Fe_2O_3, MgO, Na_2O and Ni are roughly decreasing while TiO_2, CaO, K_2O, Rb and Sr remain approximately constant in concentration. This section may represent a general fractional crystallization pattern with the exception of Al_2O_3 and Na_2O contents. The Al_2O_3 and Na_2O concentrations are predominantly affected by the crystallization of albite but a modal analysis reveals the absence of a relationship between plagioclase phenocrysts and groundmass mineral abundances and the compositional variations exhibited in the stratigraphic column. Nevertheless, it appears that the flows sampled on Ptarmigan Ridge originated from only one batch of magma. Chemical analyses for Mount Rainier are listed in Table 8.

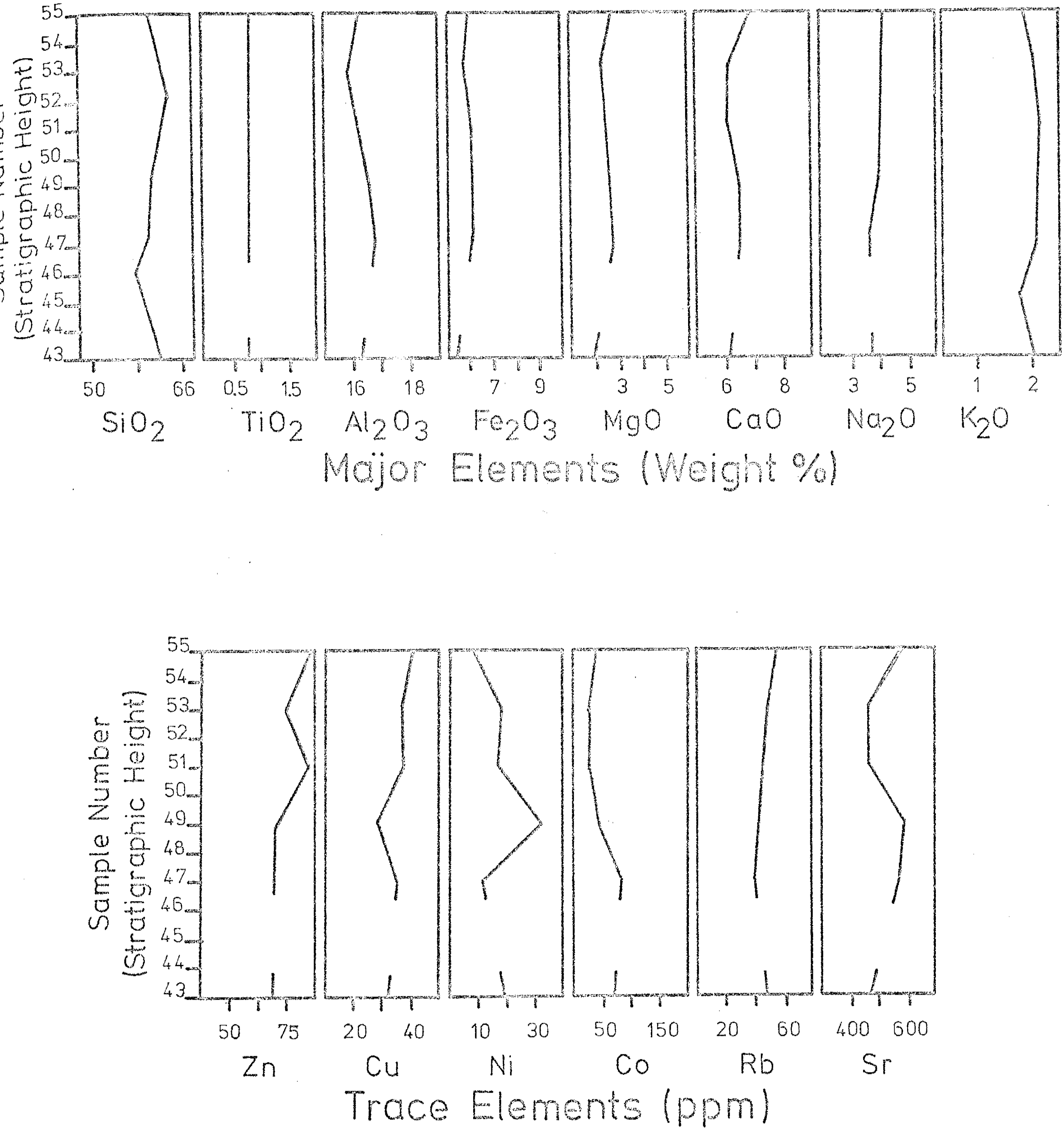

Figure 7. See following page for description.

Figure 7. The stratigraphy of Success Cleaver, Mount Rainier, compared to major and trace element compositional variations. Flow stratigraphy is represented by arbitrary vertical units. Samples from flow units having a full chemical analysis are: 29, 31, 33, 35, 37, 39, 42, 44, 46 and 49; those with only SiO_2 and K_2O concentrations are 30, 32, 36, 38, 43, 45 and 50; those without chemical analyses are 34, 40, 41, 47 and 48.

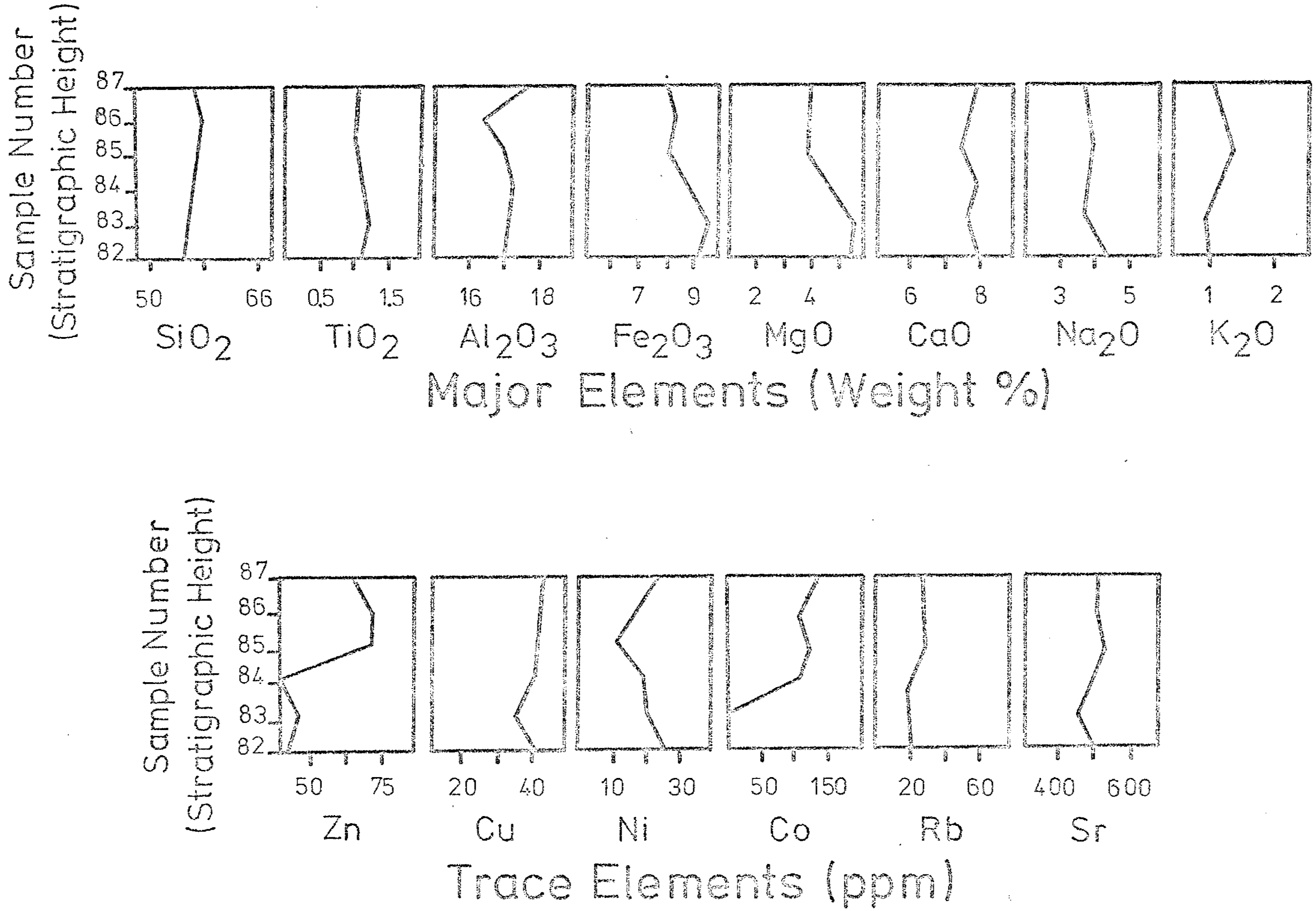

Figure 8. The stratigraphy of Ptarmigan Ridge, Mount Rainier, compared to major and trace element compositional variations. Flow stratigraphy is represented by arbitrary vertical units.

CONCLUSION AND DISCUSSION

The following conclusions that are important in the interpretations of the magma history of the lava flows of Mount Shasta, Mount Jefferson and Mount Rainier are indicated by the major and trace element data.

1. Each volcano exhibits a calc-alkaline composition that is distinct.
    a. Chemical variation diagrams reflect different chemical relationships for each volcano.
    b. Chemical variation diagrams, in general, do not exhibit smooth chemical trends as has been previously reported for these volcanoes and other calc-alkaline volcanic areas.
2. Chemical compositions generally do not vary systematically when compared in a stratigraphic section.
    a. Chemical compositions plotted with respect to stratigraphic height (age) exhibit chemical unconformities which are interpreted to delineate sub-sequences of lava flows.
    b. Chemical compositions of sub-sequences generally exhibit chemical consistency but usually do not vary systematically with the exception of Ptarmigan Ridge flows.
    c. Each sub-sequence is represented by a number of individual lava flows which probably erupted from a single batch of magma and represents a relatively

short period of time. A stratigraphic section usually contains several sub-sequences and therefore several batches of magma are represented.

d. Stratigraphic sequences or sub-sequences can exhibit systematic chemical variation if the sequence is composed of only a few lava flows in a thin stratigraphic section. Ptarmigan Ridge is an example where the chemistry of the flows, with respect to stratigraphic height (age), represents a possible fractional crystallization sequence. However, even in the Ptarmigan Ridge section, Al_2O_3 and Na_2O do not behave accordingly.

3. Chemical variations of lava flows in stratigraphic sections are not accompanied by similar mineralogic variations. The two generations of plagioclase phenocrysts in all three volcanoes could indicate magma mixing in a holding chamber.
4. All three volcanoes are chiefly composed of pyroxene andesite of the calc-alkaline series, however, Mount Shasta and Mount Rainier final stages of volcanic activity are represented by satellite cone eruptions of mafic lavas which are low in K_2O and Rb content. Mount Jefferson late stage andesites and dacites exhibit an increase in K_2O and Rb.

Coherent geochemical series of very uniform compositions have been reported for the Cascade volcanoes; Baker, Rainier, Hood and Jefferson; while the remaining Cascade volcanoes, including Shasta, have been classified as chemically divergent (McBirney, 1968). This classification appears valid with respect to existing data reported in literature. However, the additional data reported in this paper suggests the previous classification to be obsolete because: 1) the geochemistry presented in this paper suggests chemical variations to be non-systematic for all three volcanoes, but coherent with respect to alkali-magnesium-iron diagram (fig. 24), 2) previous sampling of Shasta, Jefferson and Rainier has been inadequate in terms of representative compositions, and 3) previous sampling has often been conducted on volcanic rocks not associated with the formation of stratovolcanoes. An example is found in the Mount Jefferson area (Green, 1968) where only eight chemical analyses are reported for 250 square miles and are considered by other authors to be representative of Mount Jefferson. With this type of chemical evaluating, continuous and systematic chemical variations can be easily misinterpreted.

The alkali-silica relationships in Mount Rainier, Mount Jefferson and some Mount Shasta lavas suggest a parent magma of high-alumina basalt which can produce basaltic andesites, andesites and dacites of calc-alkaline composition with progressively decreasing concentrations of Ti, Fe, Mg and Ni and progressively increasing concentrations of Si, Na and K. Although these chemical trends are not observed in long stratigraphic sections the Ptarmigan Ridge sequence does exhibit similar chemical relationships. The lavas of Ptarmigan Ridge are basaltic andesites and they are interpreted to form by fractional crystallization under hydrous conditions in a magma chamber at 30-40 km in depth (based on experimental work of Green and Ringwood, 1968). The resulting chemical variations could be produced by the removal of olivine and pyroxene phenocrysts. The non-systematic variation of Al and Na indicate a non-systematic development of plagioclase phenocrysts. The Ptarmigan Ridge flows represent only a small percentage of Mount Rainier flows; the remaining flows have a more complex magmatic history.

The remaining lava flows of Mount Rainier, Mount Jefferson and Mount Shasta do not exhibit systematic chemical variations as a function of height (age) and therefore a simple fractional crystallization scheme does not adequately explain magma evolution. The presence of sub-sequences, as previously suggested, indicates that the lava originated from several magma chambers. Fresh magma with different degrees of partial melting, but probably from the same mantle source area, may influence fractional crystallization in some or all of the magma chambers (also, the pH_2O will probably fluctuate in the different chambers as steam and other volatiles are vented during eruptions). Sporatic tapping of the magma chambers at different stages of fractional crystallization could produce the non-systematic chemical variations. Experimental data (Green and Ringwood, 1968; and Yoder, 1969) indicate that andesites and dacites of the calc-alkaline series could originate from subduction zone mechanisms (in or above the subduction zone) involving various degrees of partial melting of ecologite, peridotite or amphibole at approximately 80 km or less in depth under wet to dry conditions.

Mount Shasta andesites and basalts associated with Shastina and late stage eruptions appear to be tholeiitic in composition. Although many of the elements exhibit wide chemical variations, crustal contamination is negligible based on Sr^{87}/Sr^{86} ratios averaging 0.703 (Peterman et al., 1970). Several authors (Taylor, 1969; Tatsumoto and

Knight, 1969; Green and Ringwood, 1966; and Armstrong, 1968) propose that tholeiitic magmas may originate from the melting of the oceanic lithosphere in a subducting zone. The resulting magma may be produced by reactions involving the breakdown of amphibole at shallow depths (Fitton, 1971). The coexistence of tholeiitic and calc-alkaline rocks is commonly associated with island arc development as observed on Fiji (Gill, 1970) but generally the tholeiitic lavas precede calc-alkaline lavas. More data is required to fully evaluate this relationship at Mount Shasta as well as the late stage mafic lavas of Mount Rainier. Although it is probable that separate source areas and conduit systems would be required in the evolution of the younger mafic lavas in areas of predominantly calc-alkaline volcanism.

The data presented in this paper indicates that the Cascade magmatic evolution is extremely complex. Stratovolcanoes like Mount Shasta, Mount Jefferson and Mount Rainier need extensive sampling and chemical analyses to interpret their histories.

REFERENCES CITED

Armstrong, R. L., 1971, Isotopic and chemical constraints on models of magma genesis in volcanic arcs: Earth and Planetary Sci. Letters, v. 12, p. 137-142.

Baker, P. E., 1968, Petrology of Mount Misery volcano, St. Kitts, West Indies: Lithos, v. 1, No. 2, p. 124-150.

Callaghan, E., 1933, Some features of the volcanic sequence in the Cascade Range in Oregon: Am. Geophys. Union Trans., 14th Ann. Mtg., p. 243-249.

Ewart, A., and Stipp, J. J., 1968, Petrogenesis of the volcanic rocks of the Central North Island, New Zealand, as indicated by a study of Sr^{87}/Sr^{86} ratios, and Sr, Rb, U and Th abundances: Geochim. et Cosmochim. Acta, v. 32, p. 699-736.

Ewart, A., Taylor, S. R., and Capp, Annette C., 1968, Trace and minor element geochemistry of the tholeiitic volcanic rocks, Central North Island, New Zealand: Contr. Mineral. and Petrol., v. 18, p. 76-104.

Fiske, R. S., Hopson, C. A., and Waters, A. C., 1963, Geology of Mount Rainier National Park, Washington: U.S. Geol. Survey Prof. Paper 444, 93 p.

Fitton, J. G., 1971, The generation of magmas in island arcs: Earch and Planetary Sci. Letters, v. 11, p. 63-137.

Gill, James B., 1970, Geochemistry of Viti Levu, Fiji, and its evolution as an island arc: Contr. Mineral. and Petrol., v. 27, p. 179-203.

Gorshkov, G. S., 1969, Geophysics and petrochemistry of andesite volcanism of the circum-Pacific belt: Proceedings of the Andesite Conference, Bull. 65 (State of Oregon), p. 91.

Green, T. H., and Ringwood, A. E., 1966, Origin of the calc-alkaline igneous rock suit: Earth and Planetary Sci. Letters, v. 1, p. 307-316.

Green, T. H., and Ringwood, A. E., 1968, Genesis of the calc-alkaline igneous rock suite: Contr. Mineral. and Petrol., v. 18, p. 105-162.

Greene, R. C., 1968, Petrography and petrology of volcanic rocks in the Mount Jefferson area High Cascade Range, Oregon: U.S. Geol. Survey Bull. 1251-G, 48 p.

Hart, S. R., Brooks, C., Krogh, T. E., Davis, G. L., and Nava, D., 1970, Ancient and modern volcanic rocks: A trace element model: Earth and Planetary Sci. Letters, v. 10, p. 17-28.

Hague, A., and Iddings, J. P., 1883, Notes on the volcanoes of Northern California, Oregon and Washington Territory: Am. Jour. Sci., v. 26, p. 222-235.

Hodge, E. T., 1925, Geology of Mount Jefferson (Oregon): Mazama, Ann. Ser., v. 26, p. 222-235.

Hopson, C. A., Crowder, D. F., Tabor, R. W., Cater, F. W., and Wise, W. S., 1965, Association of andesitic volcanoes in the Cascade Mountains with Late Tertiary epizonal plutons: Geol. Soc. America Ann. Mtg., p. 79.

Jakes, P., and Gill, J., 1970, Rare earth elements and the island arc tholeiitic series: Earth and Planetary Sci. Letters, v. 9, p. 17-28.

Jakes, P., and Smith, I. E., 1970, High potassium calc-alkaline rocks from Cape Nelson, Eastern Papua: Contr. Mineral. and Petrol., v. 28, p. 259-271.

Jakes, P., and White, A. J. R., 1970, K/Rb ratio of rocks from island arcs: Geochim. et Cosmochim. Acta, v. 34, p. 849-856.

Jakes, P., and White, A. J. R., 1972, Major and trace element abundances in volcanic rocks of orogenic areas: Pre-Print.

Kuno, H., 1962, Catalogue of the active volcanoes and solfatara field of Japan, Taiwan, and Marianas, Part II.

Kuno, H., 1966, Lateral variation of basalt magma type across continental margins and island arcs: Bull. Volc., p. 29.

Kuno, Hisashi, 1969, Andesite in time and space: Proceedings of the Andesite Conference, Bull. 65 (State of Oregon), p. 13.

Lowder, G. G., and Carmichael, I. S. E., 1970, The volcanoes and caldera of Talasea, New Britain, geology and petrology: Geol. Soc. America Bull., v. 81, p. 17-38.

McBirney, Alexander R., 1968, Petrochemistry of Cascade andesite volcanoes: Andesite Conference Guidebook, Bull. 62 (State of Oregon)

McBirney, Alexander R., 1969, Compositional variations in Cenozoic calc-alkaline suites of Central America: Proceedings of the Andesite Conference, Bull. 65 (State of Oregon), p. 185.

McKee, B., 1972, Cascadia: The evolution of the Pacific Northwest: McGraw-Hill Publishers, New York, p. 394.

Mooser, F., Meyer-Abich, H., and McBirney, A. R., 1958, Catalogue of active volcanoes, part 6, Central America, p. 1-146.

Peck, D. L., Griggs, A. B., Schlicker, H. G., Wells, F. G., and Dole, H. M., 1964, Geology of the central and northern parts of the western Cascade Range in Oregon: U.S. Geol. Survey Prof. Paper 449, 56 p.

Peterman, Z. E., Carmichael, I. S. E., and Smith, A. L., 1970, Sr^{87}/Sr^{86} ratios of quaternary lavas of the Cascade range, northern California: Geol. Soc. America Bull., v. 81, p. 311-318.

Pushkar, Paul, 1968, Strontium isotope ratios in volcanic rocks of three island arc areas: Jour. Geophys. Research, v. 73, No. 8, p. 2701-2714.

Siegers, A., Richler, H., and Zeil, W., 1969, Trace element abundances in the "andesite" formation of northern Chile: Geochim. et Cosmochim. Acta, v. 33, p. 882-887.

Shaw, D. M., 1968, A review of K-Rb fractionation trends by covariance analysis: Geochim. et Cosmochim. Acta, v. 32, p. 573-602.

Smith, A. L., and Carmichael, I. S. E., 1968, Quaternary lavas from the Southern Cascades, Western U.S.A.: Contr. Mineral. and Petrol., v. 19, No. 3, p. 212-238.

Tatsumoto, M., and Knight, R. J., 1969, Lead in tholeiitic and high-alumina basalts from Central Japan (Abstract): Proceedings of the Andesite Conference, Bull. 65 (State of Oregon), p. 191.

Taylor, S. R., 1969, Trace element chemistry of andesites and associated calc-alkaline rocks: Ore. Dept. Geol. and Min. Ind. Bull., v. 65, p. 43-64.

Taylor, S. R., Capp, C., Graham, A. L., and Blake, D. H., 1969a, Trace element abundances in andesites: Contr. Mineral. and Petrol., v. 23, p. 1-26.

Taylor, S. R., Kay, Maureen, White, A. J. R., Duncan, A. R., and Ewart, A., 1969b, Genetic significance of Co, Cr, Ni, Sc and U content of andesites: Geochim. et Cosmochim. Acta, v. 33, p. 275-286.

Taylor, S. R., and White, A. J. R., 1966, Trace element abundances in andesites: Bull. Volcanology, v. 29, p. 177-194.

Thayer, T. P., 1937, Petrology of later Tertiary and Quaternary rocks of the north central Cascade Mountains in Oregon: Geol. Soc. America Bull., v. 48, p. 1611-1652.

Thayer, T. P., 1939, Geology of the Salem Hills and the North Santiam River Basin, Oregon: Ore. Dept. Geol. and Min. Ind. Bull., v. 15, 40 p.

Walker, G. W., Greene, R. C., and Pattee, E. C., 1966, Mineral resources of the Mt. Jefferson Primitive Area, Oregon: U.S. Geol. Survey Bull. 1230-D, 32 p.

Williams, H., 1932a, Geology of the Lassen Volcanic National Park, California: Calif. Univ., Dept. Geol. Sci., Bull. 21, p. 195-385.

Williams, H., 1932b, Mt. Shasta, a Cascade volcano: Jour. Geology, v. 40, No. 5, p. 417-429.

Williams, Howel, 1934, Mount Shasta, California: Zeitschr. Vulkanolgie, v. 15, p. 225-253.

Williams, H., 1942, The geology of Crater Lake National Park, Oregon: Carnegie Inst. Wash. Publ. 540.

Wise, Williams S., 1969, Geology and petrology of the Mt. Hood area: a study of high Cascade volcanism: Geol. Soc. America, v. 80, p. 969-1004.

Yoder, H. S. (Jr.), 1969, Calc-alkaline andesites: experimental data bearing on the origin of their assumed characteristics: Proceedings of the Andesite Conference, Bull. 65 (State of Oregon), p. 77.

APPENDIX

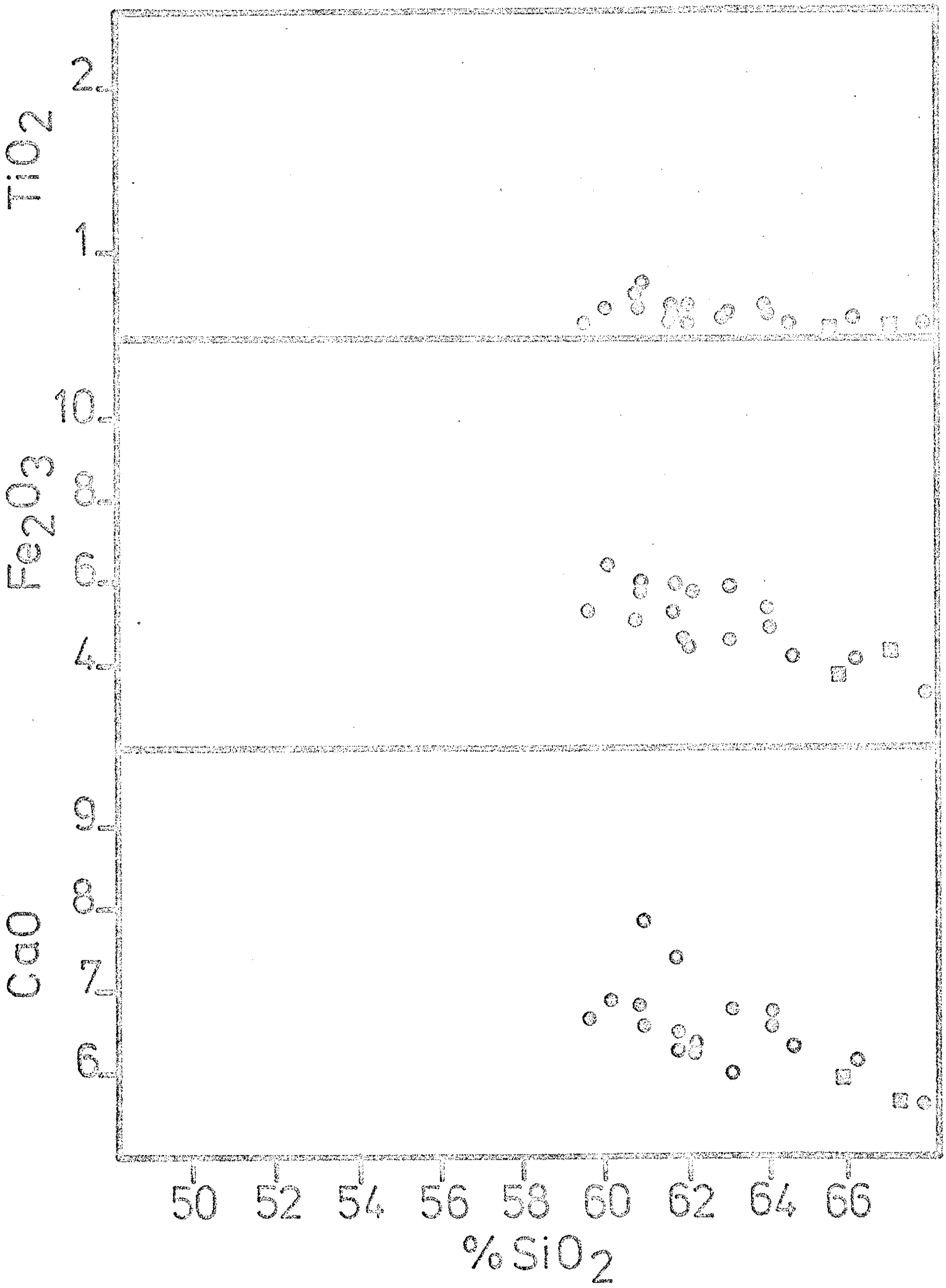

Figure 9. See following page for description.

Figure 9. Major element (TiO_2, Fe_2O_3 and CaO) SiO_2 variation diagram for Mount Shasta volcanic rocks, oxides in weight percent. Symbols: ⊙ = Mount Shasta andesite; o = Shastina andesite and dacite; ⊡ = domes and plugs.

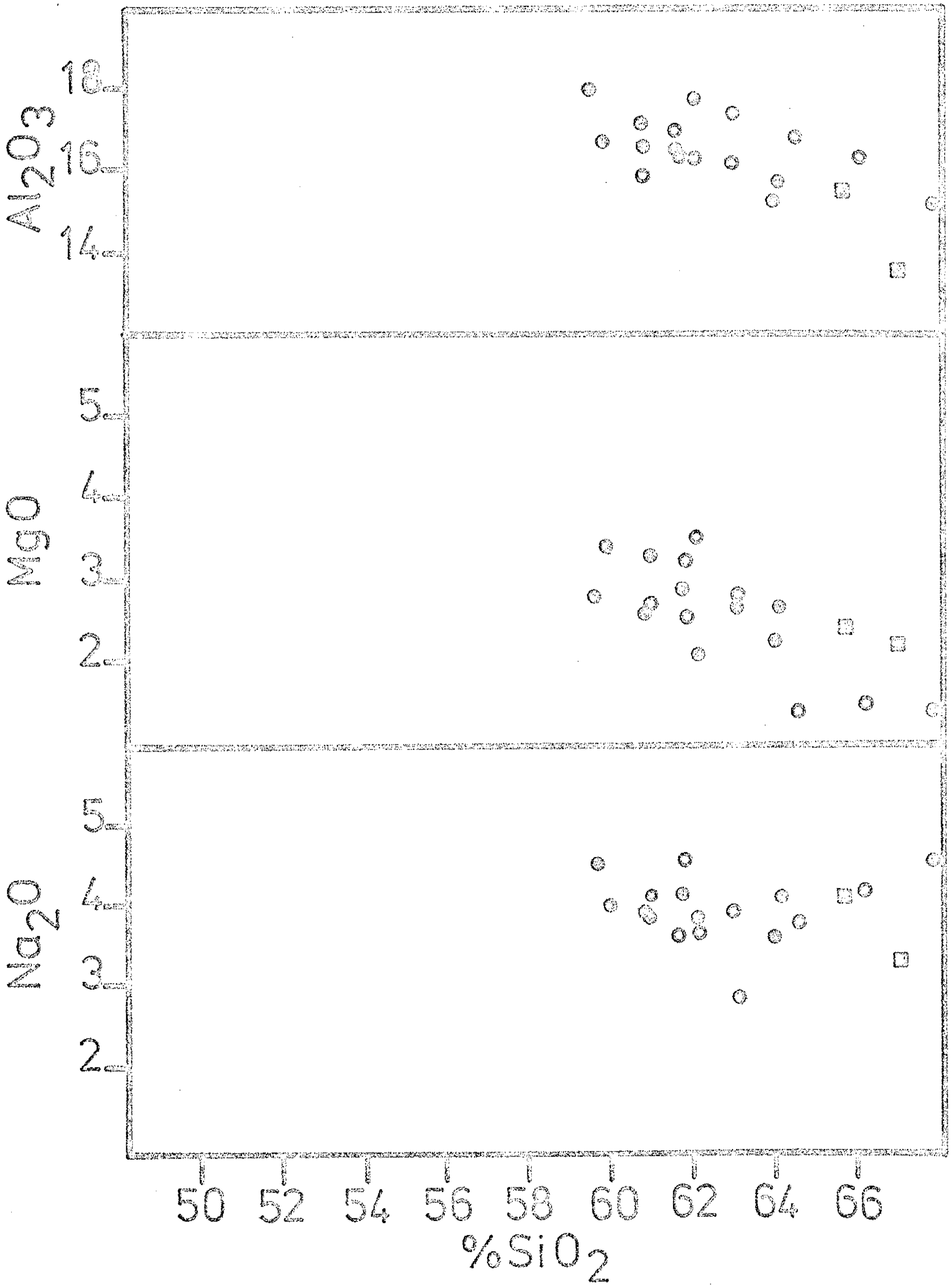

Figure 10. See following page for description.

Figure 10. Major element (Al_2O_3, MgO and Na_2O) SiO_2 variation diagram for Mount Shasta volcanic rocks, oxides in weight percent. Symbols: ⊘ = Mount Shasta andesite; o = Shastina andesite and dacite; ▨ = domes and plugs.

Figure 11. Trace element (Zn, Cu and Ni) SiO_2 variation diagram for Mount Shasta volcanic rocks, elements in ppm and SiO_2 in weight percent. Symbols: ⊖ = Mount Shasta andesite; ○ = Shastina andesite and dacite; ▨ = domes and plugs.

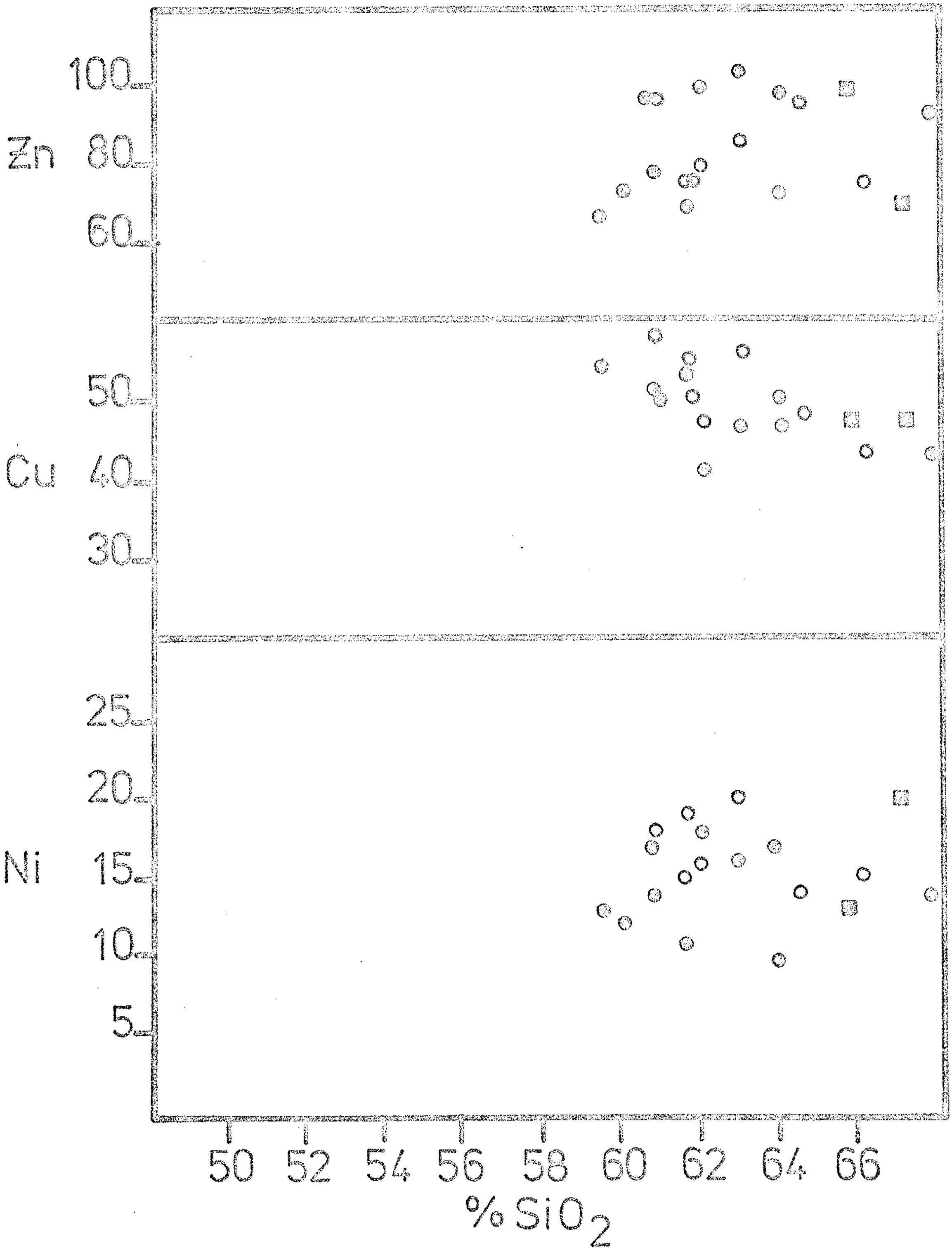

Figure 12. Trace element (Co, Rb and Sr) SiO_2 variation diagram for Mount Shasta volcanic rocks, elements in ppm and SiO_2 weight percent. Symbols: ⊙ = Mount Shasta andesite; o = Shastina andesite and dacite; ▨= domes and plugs.

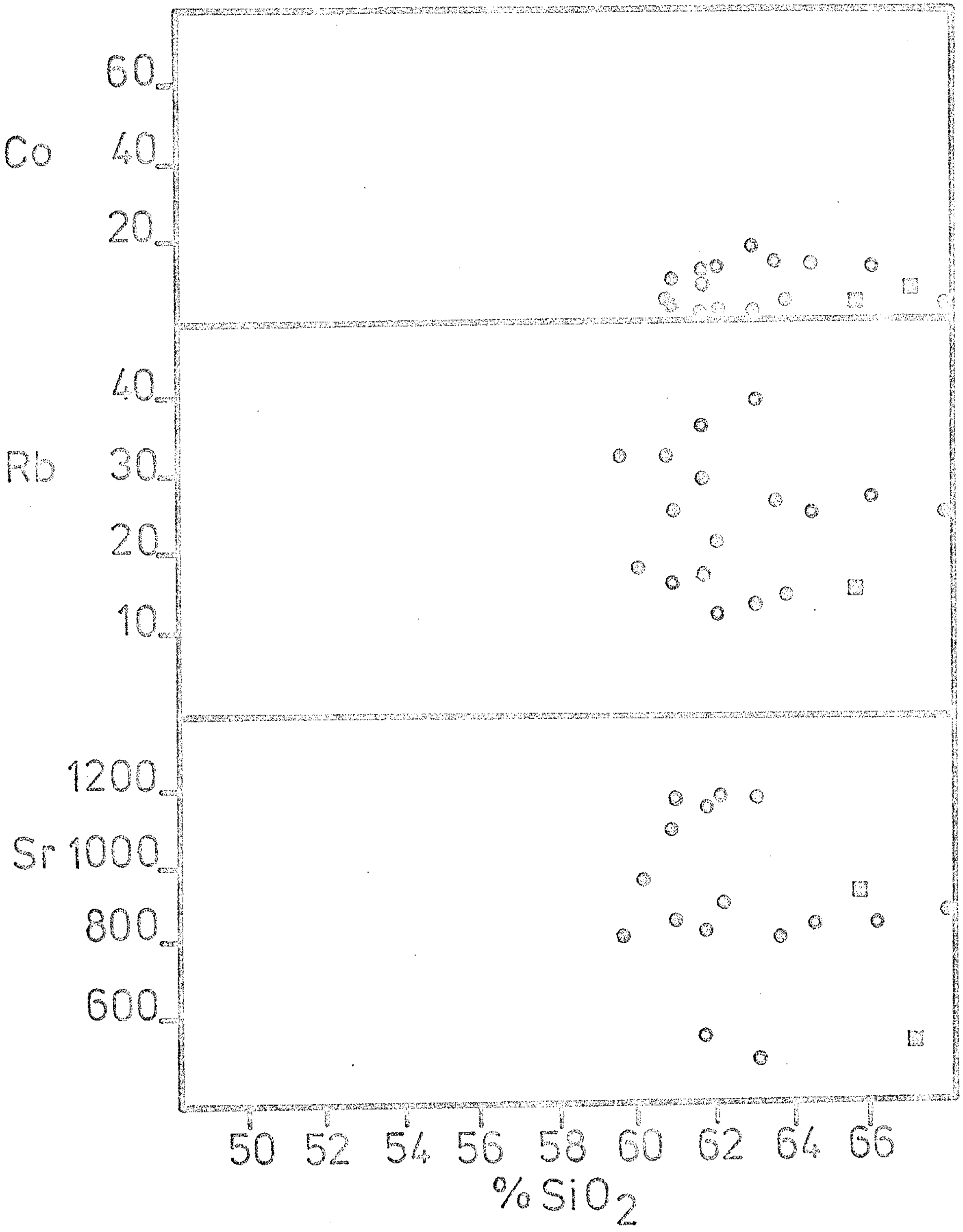

Figure 13. Major element (TiO_2, Fe_2O_3 and CaO) SiO_2 variation diagram for Mount Jefferson volcanic rocks, oxides in weight percent.

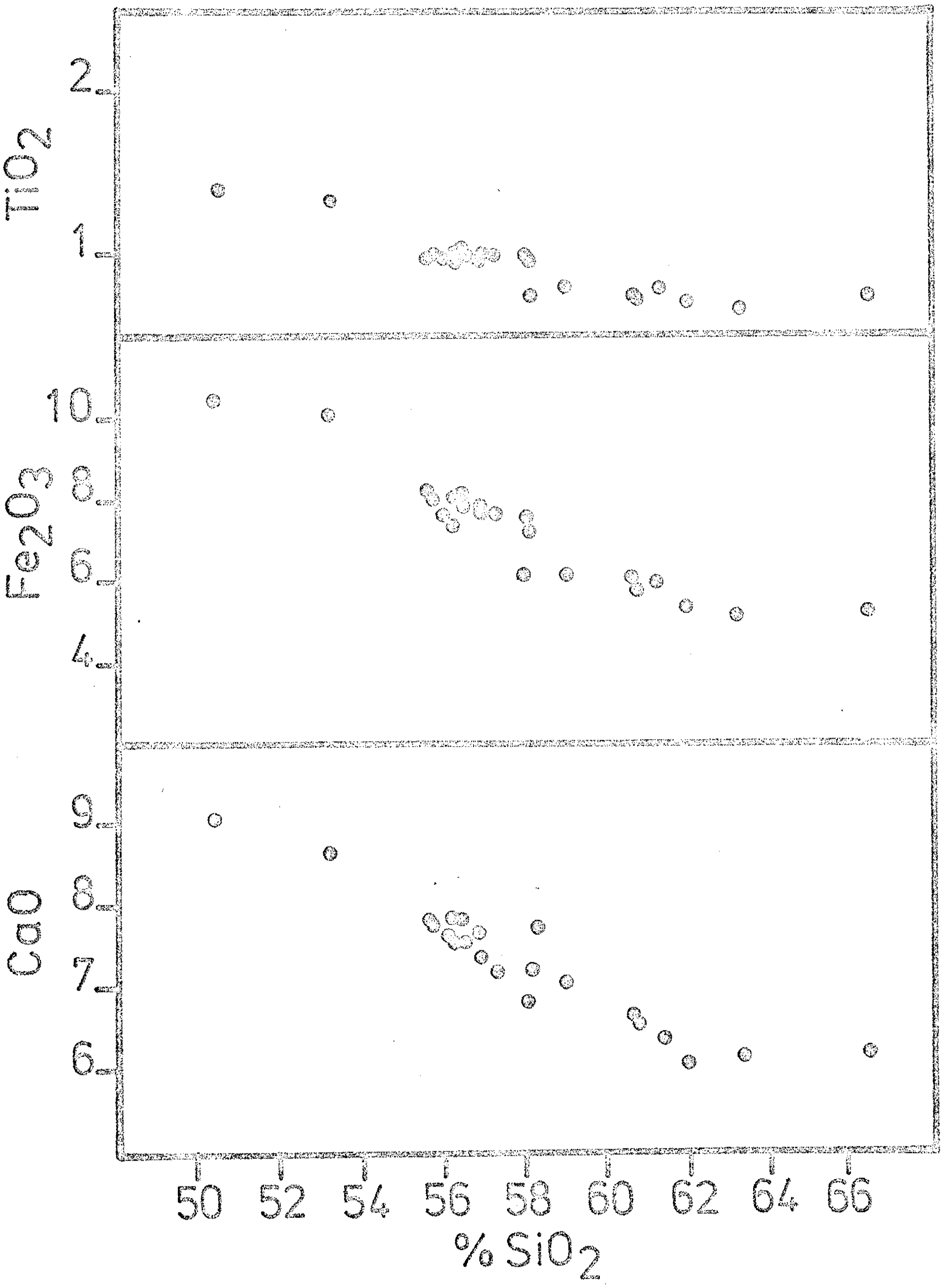

Figure 14. Major element (Al_2O_3, MgO and Na_2O) SiO_2 variation diagram for Mount Jefferson volcanic rocks, oxides in weight percent.

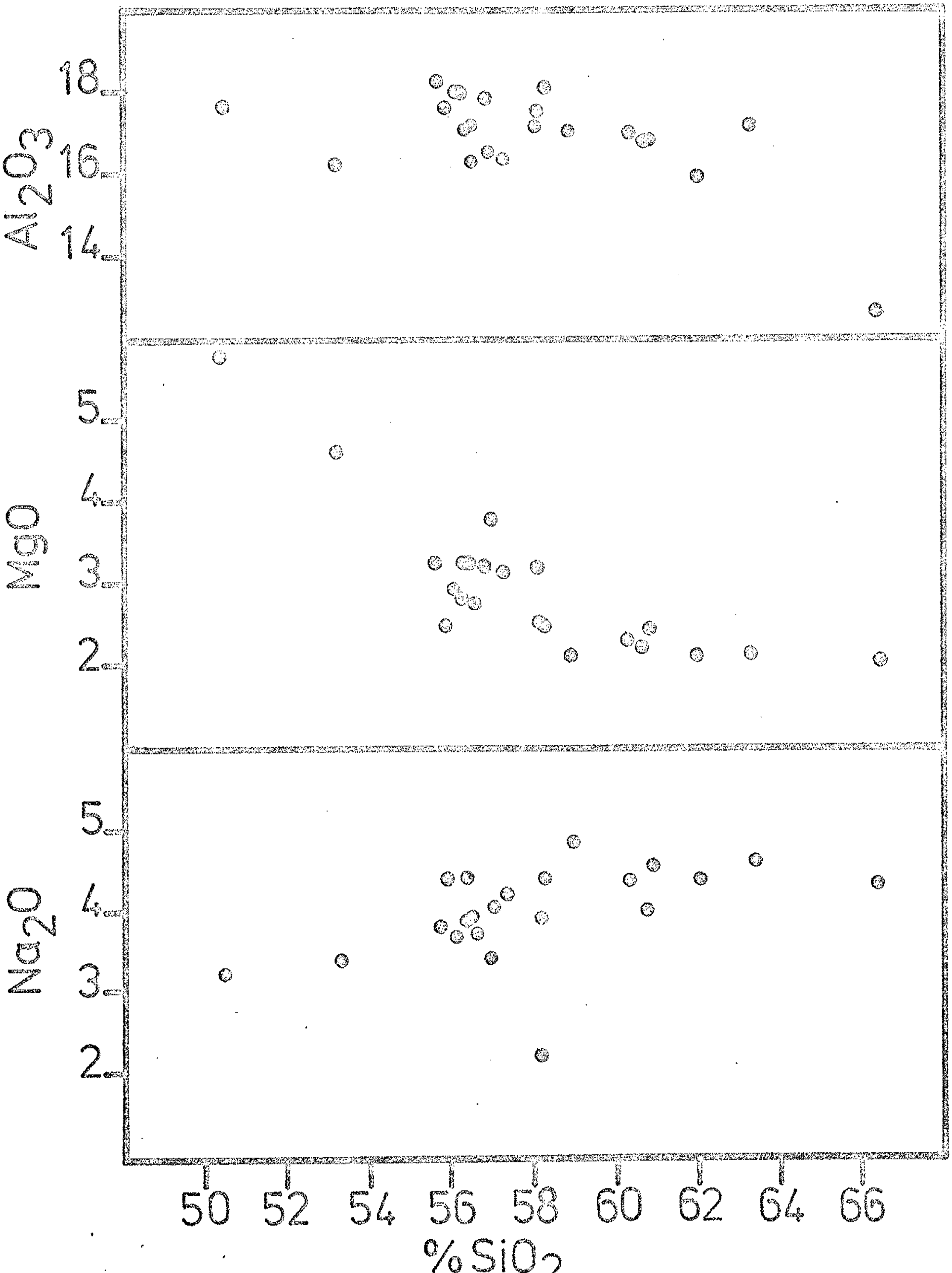

Figure 15. Trace element (Zn, Cu and Ni) SiO_2 variation diagram for Mount Jefferson volcanic rocks, elements in ppm and SiO_2 in weight percent.

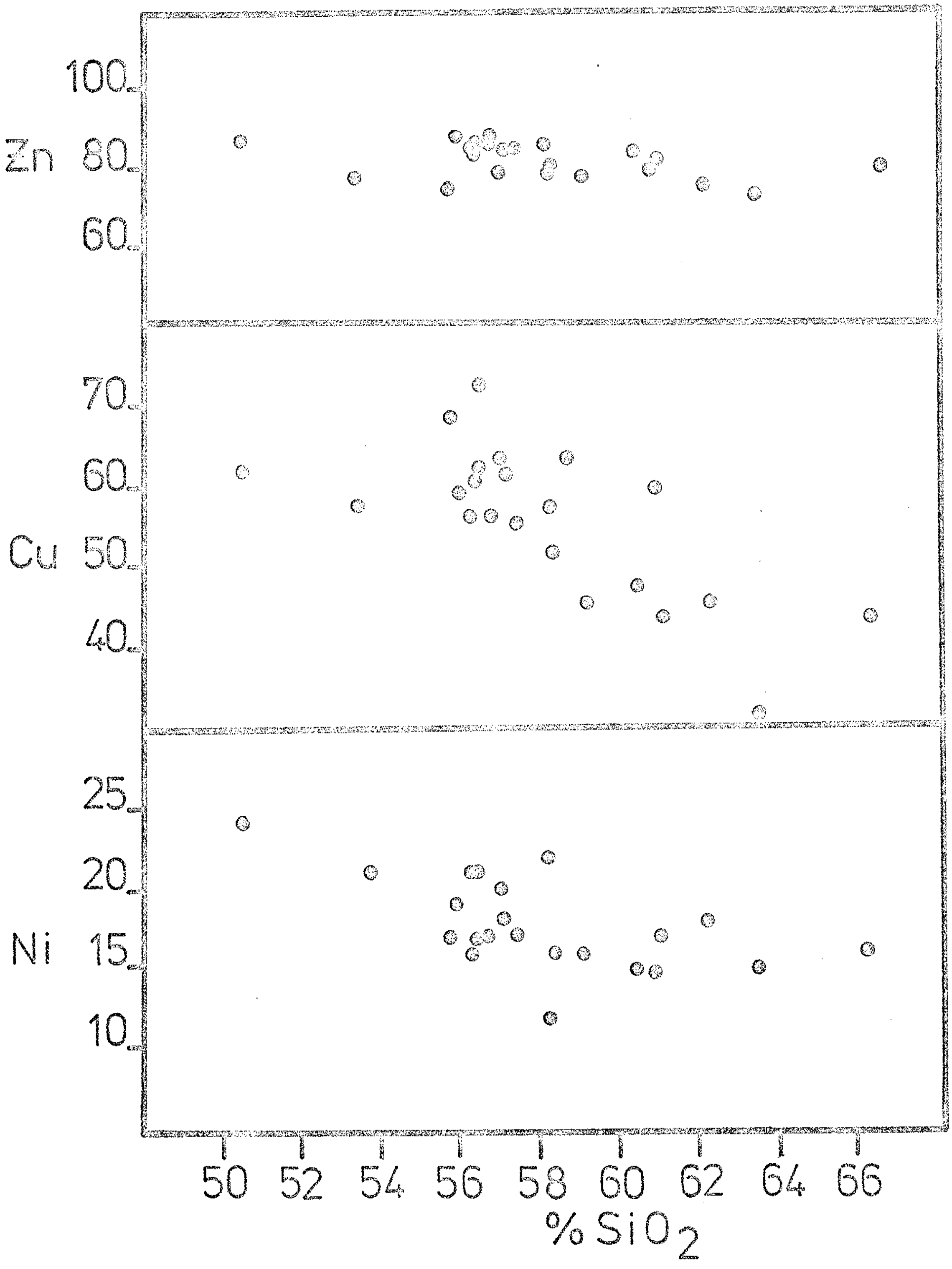

Figure 16. Trace element (Co, Rb and Sr) SiO_2 variation diagram for Mount Jefferson volcanic rocks, elements in ppm and SiO_2 in weight percent.

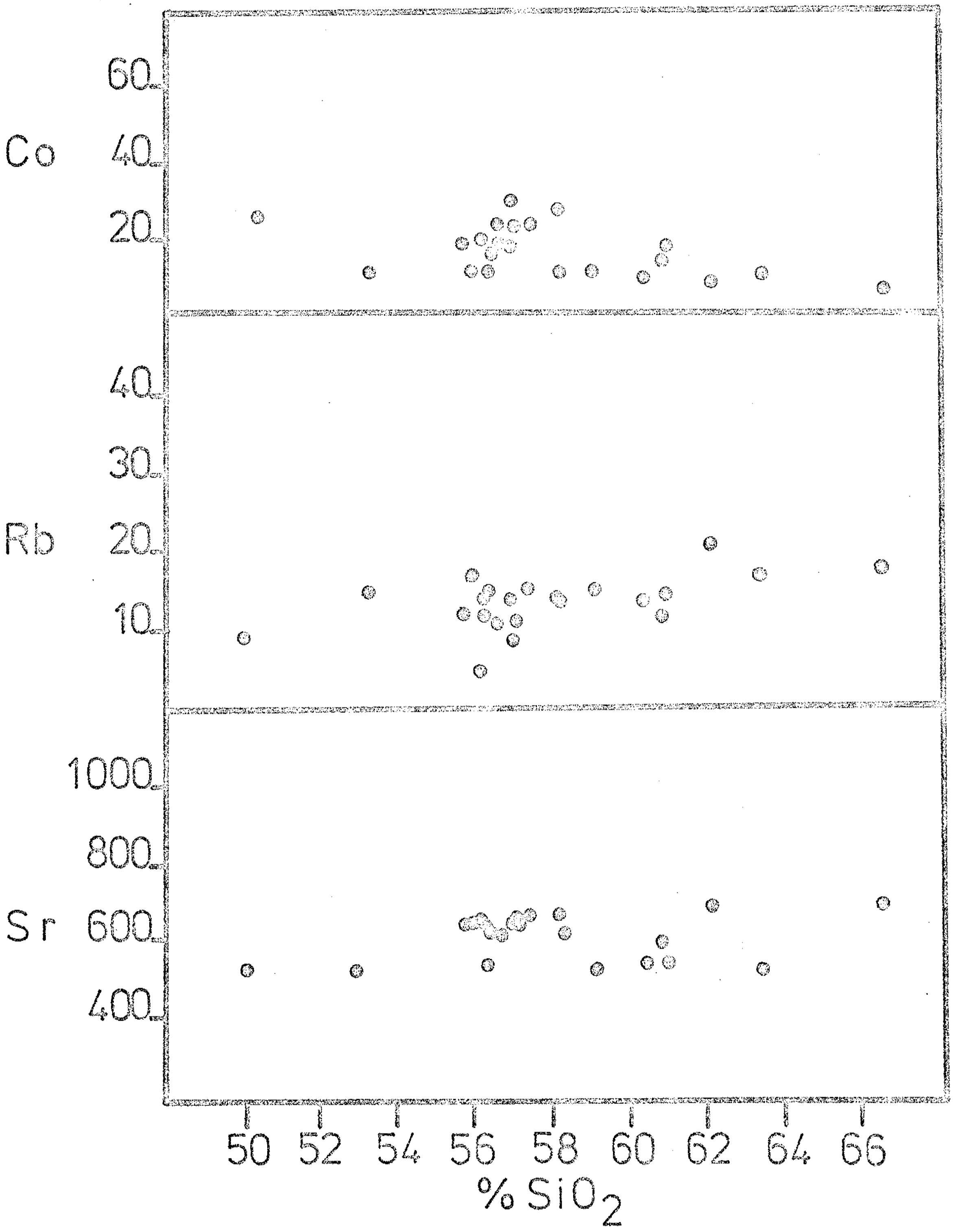

Figure 17. Major element (TiO_2, Fe_2O_3 and CaO) SiO_2 variation diagram for Mount Rainier volcanic rocks, oxides in weight percent. Symbols: ▨ = young basaltic andesite; ● = andesite and dacite.

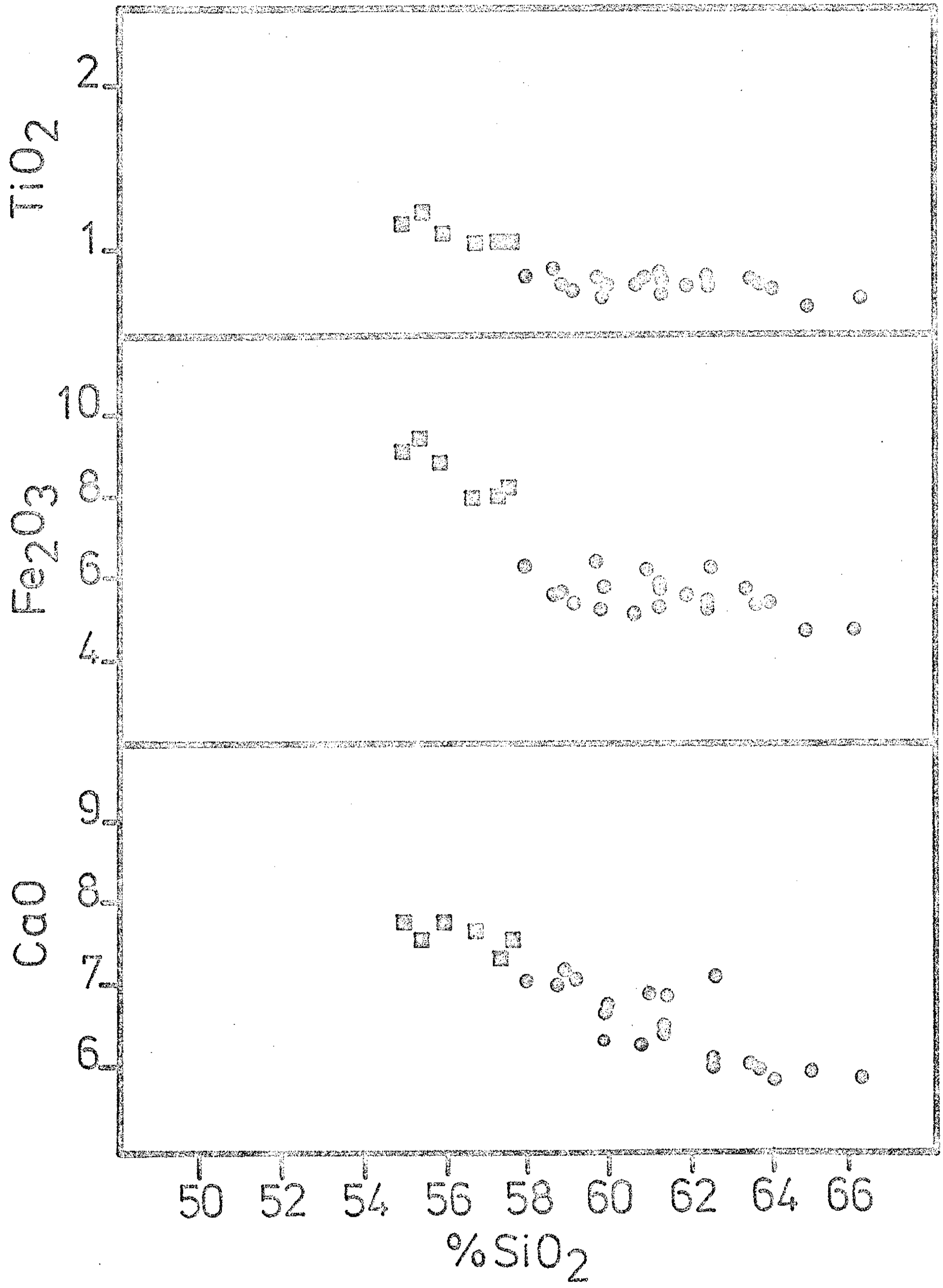

Figure 18. Major element (Al_2O_3, MgO and Na_2O) SiO_2 variation diagram for Mount Rainier volcanic rocks, oxides in weight percent. Symbols: ▨ = young basaltic andesite; ● = andesite and dacite.

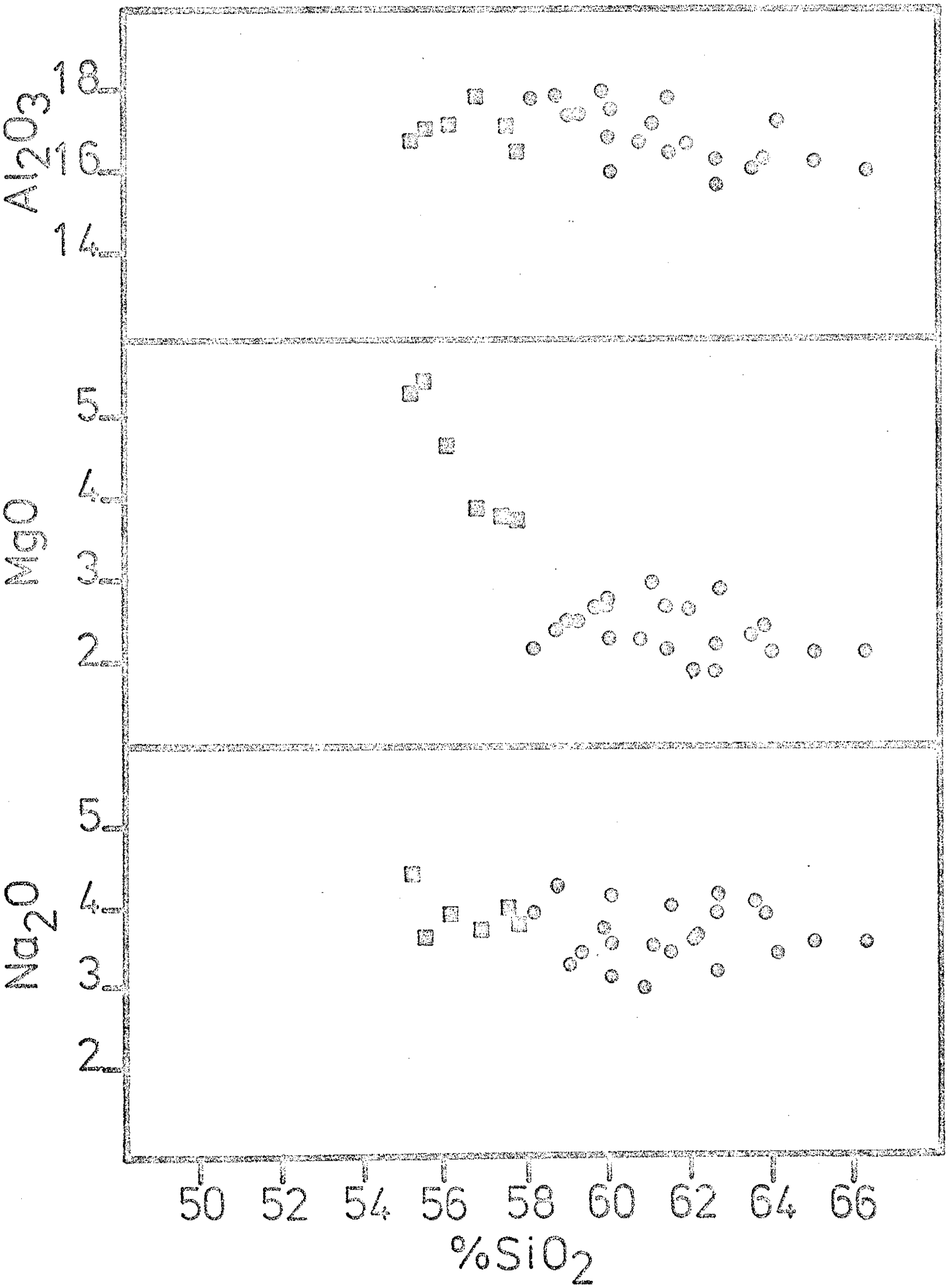

Figure 19. Trace element (Zn, Cu and Ni) SiO_2 variation diagram for Mount Rainier volcanic rocks, elements in ppm and oxides in weight percent. Symbols: ▨ = young basaltic andesite; ● = andesite and dacite.

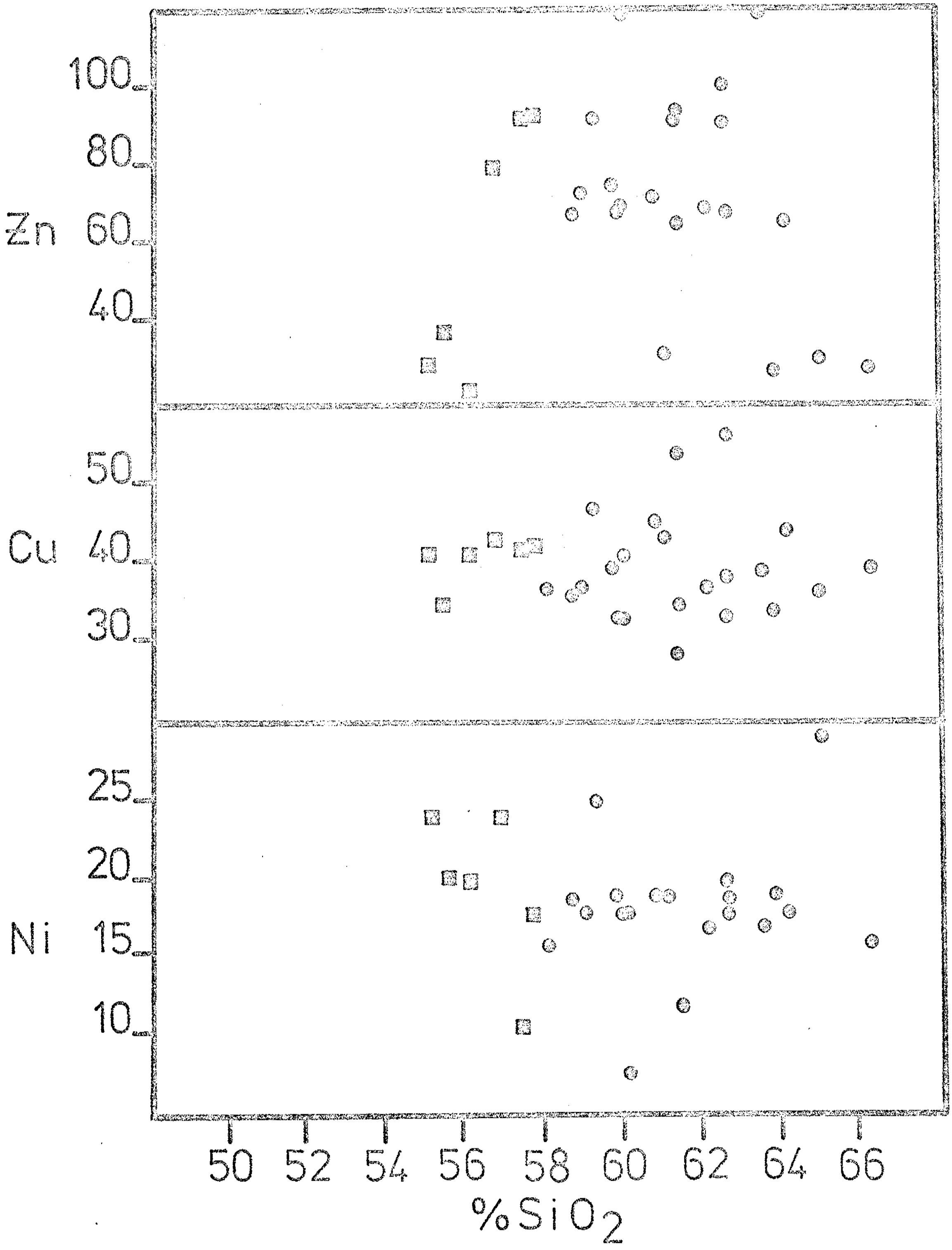

Figure 20. Trace element (Co, Rb and Sr) SiO_2 variation diagram for Mount Rainier volcanic rocks, elements in ppm and oxides in weight percent. Symbols: ▨ = young basaltic andesite; ● = andesite and dacite.

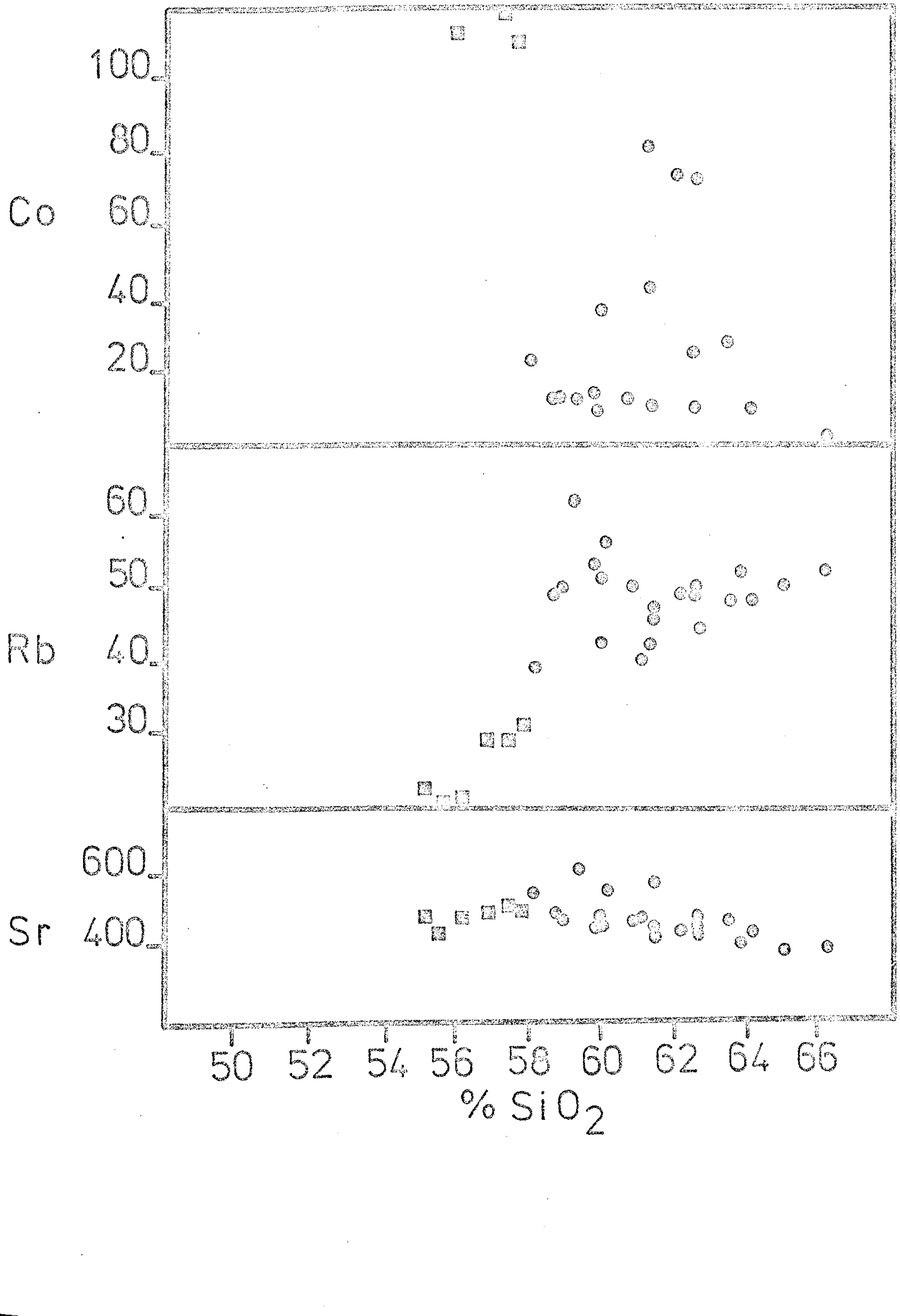

Figure 21. See following page for description.

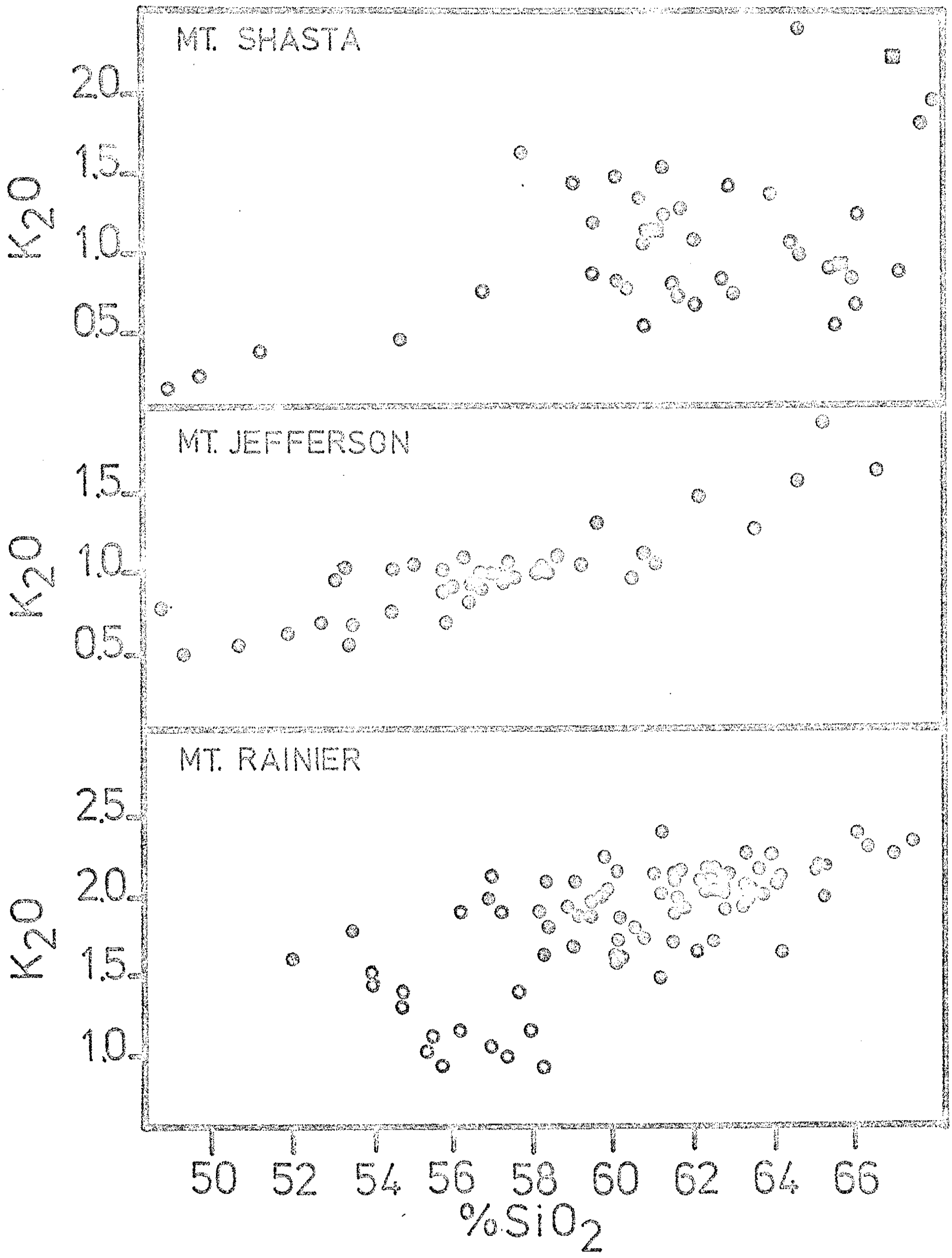

Figure 21. K_2O-SiO_2 variation diagram for Mount Shasta, Mount Jefferson and Mount Rainier, oxides in weight percent. Symbols: Mount Shasta, ● = Mount Shasta andesite, o = Shastina basalt andesite and dacite, ▨ = domes and plugs; Mount Jefferson, ● = andesite and dacite; Mount Rainier, o = young basaltic andesite, ● = andesite and dacite.

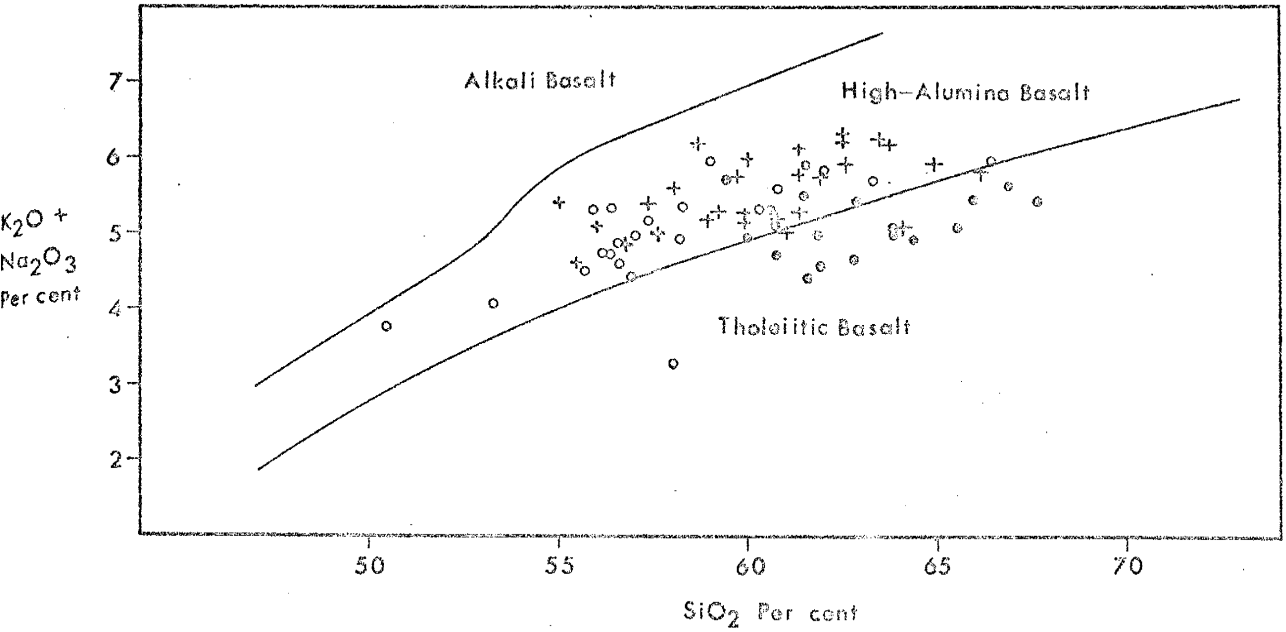

Figure 22. Variation diagram of total alkalies and SiO_2, oxides in weight percent. Basaltic divisions on diagram were taken from Kuno (1966, 1969). Symbols: o = Mount Shasta volcanic rocks; o = Mount Jefferson volcanic rocks; + = Mount Rainier volcanic rocks.

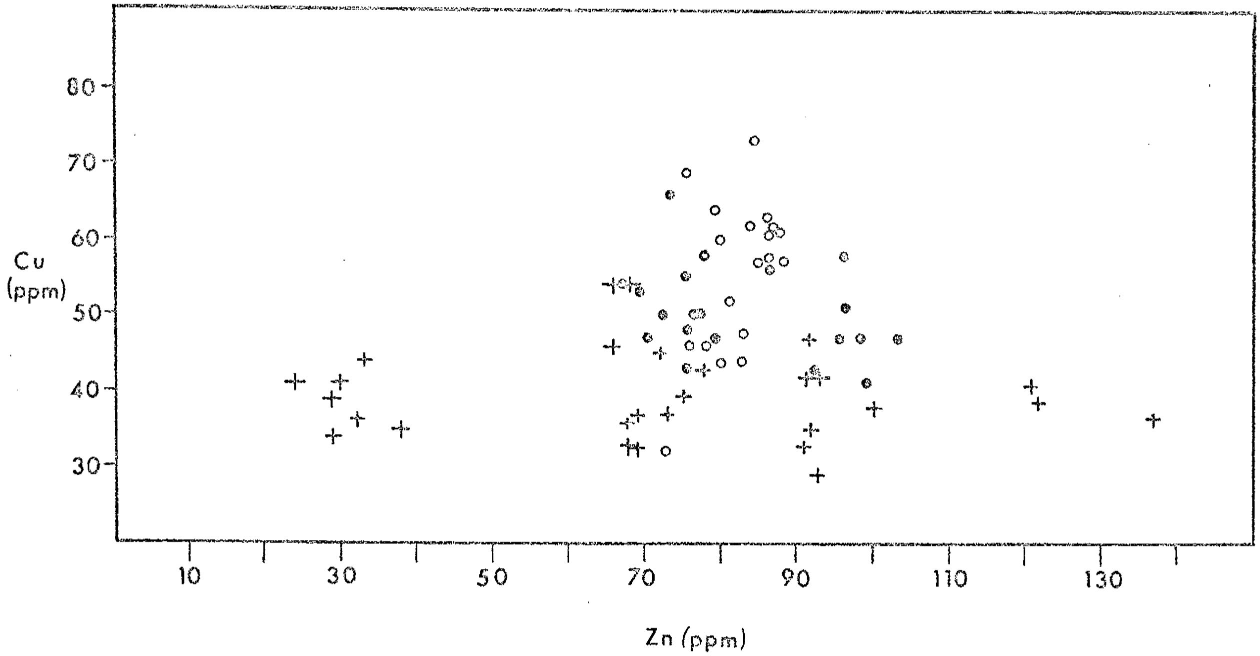

Figure 23. Variation diagram of copper and zinc, elements in ppm. Symbols: o = Mount Shasta volcanic rocks; o = Mount Jefferson volcanic rocks; + = Mount Rainier volcanic rocks.

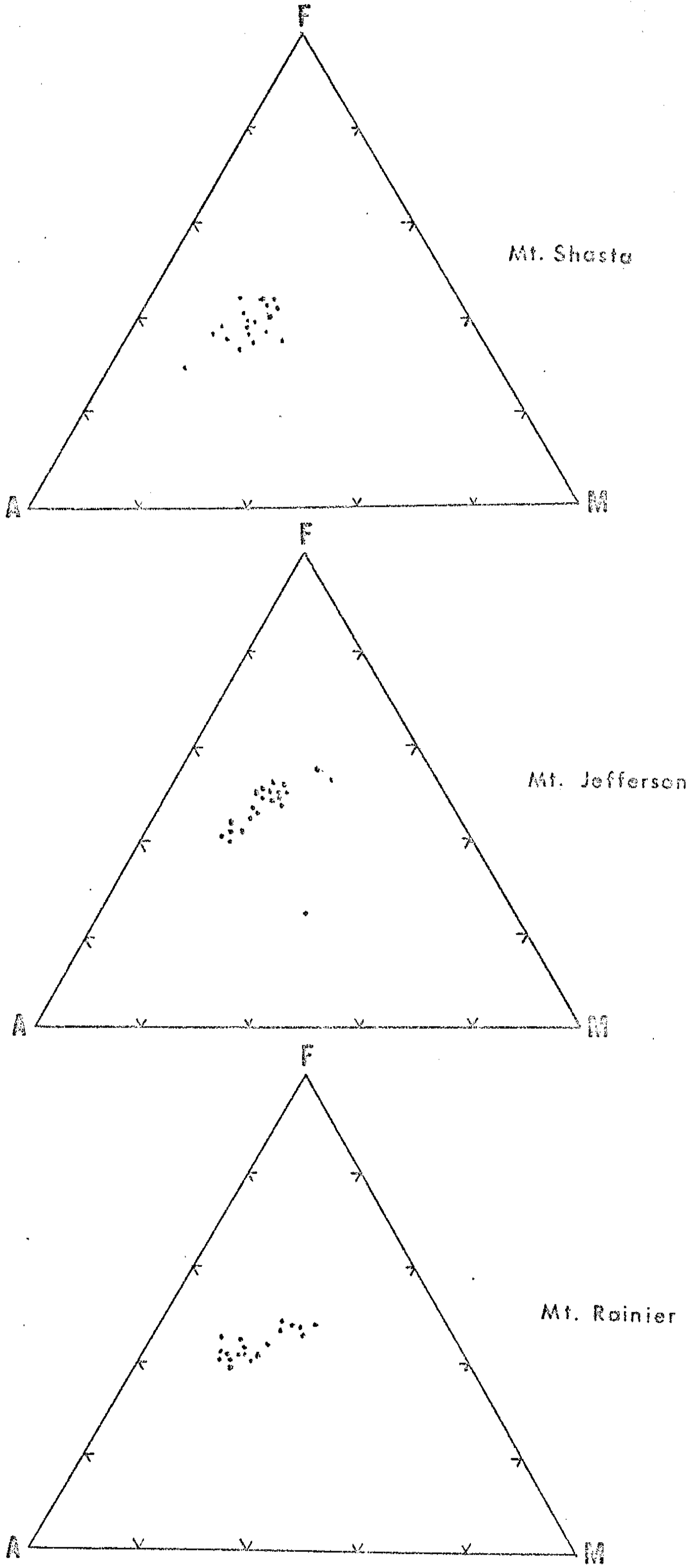

Figure 24. See following page for description.

Figure 24. Alkali-Magnesium-Iron (AMF) ternary diagrams for Mount Shasta, Mount Jefferson and Mount Rainier. Alkalies = Na_2O + K_2O weight percent and total iron is expressed in Fe_2O_3 weight percent.

Table 6. Chemical Analyses of Mount Shasta Lava Flows

Major Elements	S04	S09	S13	S14	S15	S17	S18
SiO_2	57.54	54.47	59.39	61.48	59.93	60.70	63.79
TiO_2			.59	.59	.67	.68	.70
Al_2O_3			18.01	16.61	16.74	16.55	15.30
Fe_2O_3			5.26	4.62	6.42	5.74	5.15
MgO			2.84	2.92	3.45	3.31	2.33
CaO			6.70	6.52	6.90	6.61	6.59
Na_2O			4.55	4.20	4.08	3.92	3.68
K_2O	1.64	.49	1.18	1.30	.83	1.16	1.37
Total			98.52	98.24	99.01	98.67	98.91
Trace Elements							
Zn			67	69	73	77	72
Cu			54	53	66	50	50
Ni			13	11	12	14	17
Rb			33	30	19	26	27
Sr			834	842	965	862	833
Co			Tr	2	Tr	11	15
Element Ratios							
K/Rb			297	360	363	370	421
Sr/Rb			25.3	28.1	50.8	33.2	30.8
K/Sr			11.6	12.8	7.14	11.2	14.1
Ca/Sr			57.47	55.34	51.10	54.80	56.54
Zn/Cu			1.60	1.64	1.06	2.08	2.32

Table 6. (continued)

Major Elements	S21	S24	S25	S26	S28	S30	S31
SiO_2	66.92	61.47	67.03	58.88	65.25	61.88	62.85
TiO_2	.56	.68				.71	.65
Al_2O_3	13.54	16.88				17.79	17.46
Fe_2O_3	4.27	5.19				5.70	4.56
MgO	2.18	2.59				2.09	2.71
CaO	5.64	7.38				6.66	6.83
Na_2O	3.36	3.66				3.92	2.94
K_2O	2.27	.75	.89	1.44	.90	1.08	.75
Total	98.74	98.60				99.83	98.75
Trace Elements							
Zn	70	75				99	103
Cu	47	55				41	47
Ni	20	15				18	16
Rb	65	18				22	14
Sr	577	1164				919	1195
Co	9	10				3	3
Element Ratios							
K/Rb	290	346				408	445
Sr/Rb	8.88	64.7				41.8	85.4
K/Sr	32.7	5.35				9.76	5.21
Ca/Sr	69.86	45.31				51.79	40.84
Zn/Cu	1.52	1.63				6.19	3.68

Table 6. (continued)

Major Elements	S32	S33	S34	S35	S36	S37	S39
SiO_2	61.09	64.52	60.60	63.86	59.93	65.55	61.28
TiO_2			.77	.72		.50	
Al_2O_3			17.16	15.76		15.48	
Fe_2O_3			5.15	4.98		3.66	
MgO			2.62	2.72		2.44	
CaO			6.86	6.77		5.97	
Na_2O			4.00	4.16		4.16	
K_2O	1.54	2.39	1.34	.83	1.49	.91	.82
Total			98.50	99.80		98.67	
Trace Elements							
Zn			96	98		95	
Cu			51	47		47	
Ni			17	10		13	
Rb			33	15		16	
Sr			1100	1322		951	
Co			6	5		5	
Element Ratios							
K/Rb			337	459		472	
Sr/Rb			33.3	88.1		59.4	
K/Sr			10.1	5.21		7.94	
Ca/Sr			44.6	36.6		44.9	
Zn/Cu			2.67	2.88		2.88	

Table 6. (continued)

Major Elements	C41	S42	C43	S44	C47	S50	S51
SiO_2	49.42	48.68	56.43	51.06	59.36	67.88	60.20
TiO_2							
Al_2O_3							
Fe_2O_3							
MgO							
CaO							
Na_2O							
K_2O	.25	.18	.76	.40	.88	1.95	.77
Total							
Trace Elements							
Zn							
Cu							
Ni							
Rb							
Sr							
Co							
Element Ratios							
K/Rb							
Sr/Rb							
K/Sr							
Ca/Sr							
Zn/Cu							

Table 6. (continued)

Major Elements	S52	S53	S55	S56	S58	S59	S60
SiO_2	64.57	61.09	60.70	62.58	60.80	60.86	67.63
TiO_2			.79				.57
Al_2O_3			15.80				15.10
Fe_2O_3			5.82				3.34
MgO			2.73				1.48
CaO			7.86				5.64
Na_2O			4.14				4.63
K_2O	.98	1.25	.56	.81	1.25	1.11	1.80
Total			98.22				100.19
Trace Elements							
Zn			96				92
Cu			58				43
Ni			18				14
Rb			17				26
Sr			1180				900
Co			4				5
Element Ratios							
K/Rb			273				575
Sr/Rb			69.4				34.6
K/Sr			3.94				16.6
Ca/Sr			47.6				87.7
Zn/Cu			1.88				3.28

Table 6. (continued)

Major Elements	S61	C64	C65	S67	S68	S69	S70
SiO_2	65.96	61.88	65.34	61.56	62.82	65.94	64.35
TiO_2		.56		.61	.65	.62	.58
Al_2O_3		16.30		16.42	16.19	16.24	16.80
Fe_2O_3		4.42		4.92	4.95	4.07	4.14
MgO		3.55		3.28	2.85	1.77	1.72
CaO		6.34		6.30	6.00	6.11	6.30
Na_2O		3.84		4.63	4.00	4.24	3.84
K_2O	.65	.68	.54	1.28	1.41	1.21	1.05
Total		97.57		98.00	98.87	100.2	98.78
Trace Elements							
Zn		79		76	86	75	75
Cu		47		50	56	43	48
Ni		16		19	20	15	14
Rb		13		37	40	28	26
Sr		1196		577	519	857	864
Co		14		14	19	14	15
Element Ratios							
K/Rb		434		287	293	359	335
Sr/Rb		92.0		15.6	13.0	30.6	33.2
K/Sr		4.72		18.4	22.6	11.7	10.1
Ca/Sr		74.2		153	162	50.9	52.1
Zn/Cu		2.47		2.05	2.20	2.68	1.97

Table 7. Chemical Analyses of Mount Jefferson Lava Flows

Major Elements	F11	F15	F16	F17	F18	F19	F20
SiO_2	52.59	53.30	56.92	55.87	58.18	56.37	56.59
TiO_2		1.37	.98	1.02	.99	1.04	1.03
Al_2O_3		16.29	17.97	17.66	17.20	17.11	16.36
Fe_2O_3		10.19	7.71	8.02	7.58	8.02	7.94
MgO		4.63	3.20	2.50	2.52	2.79	2.77
CaO		8.74	7.76	7.85	7.27	7.92	7.96
Na_2O		3.42	3.44	4.42	3.92	4.42	3.71
K_2O	.66	.65	.96	.90	.99	.93	.88
Total		98.59	98.68	98.24	98.65	98.61	97.24
Trace Elements							
Zn		78	79	88	79	86	88
Cu		58	64	61	64	63	57
Ni		21	20	19	12	21	17
Rb		15	9	17	14	15	14
Sr		531	653	654	628	624	621
Co		12	29	13	12	12	19
Element Ratios							
K/Rb		360	886	439	587	481	522
Sr/Rb		35.4	72.6	46.7	44.8	41.6	44.4
K/Sr		10.2	12.2	11.4	13.1	11.6	11.8
Ca/Sr		118	84.9	85.8	82.7	90.7	91.8
Zn/Cu		1.70	1.25	1.57	1.23	1.41	1.54

Table 7. (continued)

Major Elements	F25	F27	F29	F30	F31	F32	F33
SiO_2	49.14	50.45	56.13	54.88	56.29	59.45	60.73
TiO_2		1.41	1.00		.96		.78
Al_2O_3		17.76	18.16		18.15		16.99
Fe_2O_3		10.55	7.87		7.58		6.28
MgO		5.79	2.89		3.28		2.26
CaO		9.13	7.77		7.78		6.75
Na_2O		3.26	3.71		3.92		4.00
K_2O	.50	.54	1.04	1.01	.80	1.27	1.09
Total		98.89	98.57		98.76		98.88
Trace Elements							
Zn		87	85		84		80
Cu		62	57		73		60
Ni		24	16		17		15
Rb		9	5		11		12
Sr		536	664		653		602
Co		26	20		18		15
Element Ratios							
K/Rb		498	1730		604		754
Sr/Rb		59.6	133		59.4		50.2
K/Sr		8.4	13.0		10.2		15.0
Ca/Sr		121.7	83.6		85.2		80.1
Zn/Cu		1.40	1.49		1.15		1.33

Table 7. (continued)

Major Elements	F35	F36	F37	F38	F39	F42	F43
SiO_2	60.82	57.18	58.26	55.73	58.08	56.56	57.25
TiO_2	.78		.78		1.03	1.03	
Al_2O_3	16.97		18.29		17.72	17.27	
Fe_2O_3	5.93		6.30		7.31	8.16	
MgO	2.45		2.50		3.19	3.30	
CaO	6.70		6.89		7.81	7.65	
Na_2O	4.55		4.39		2.27	3.92	
K_2O	1.03	.96	.96	.88	.97	.96	1.01
Total	99.23		98.37		98.38	98.85	
Trace Elements							
Zn	83		81		86	86	
Cu	44		52		58	61	
Ni	17		16		22	21	
Rb	15		14		15	14	
Sr	552		556		674	671	
Co	17		19		27	24	
Element Ratios							
K/Rb	570		569		537	569	
Sr/Rb	36.8		39.7		44.9	47.9	
K/Sr	15.5		14.3		11.9	11.9	
Ca/Sr	86.7		88.6		82.8	81.5	
Zn/Cu	1.89		1.56		1.48	1.41	

Table 7. (continued)

Major Elements	F44	F45	F46	F49	F50	J06	J07
SiO_2	57.00	54.38	57.34	55.70	54.31	51.70	65.09
TiO_2	1.00		1.01	1.01			
Al_2O_3	16.60		16.41	18.38			
Fe_2O_3	7.73		7.74	8.34			
MgO	3.77		3.11	3.28			
CaO	7.42		7.29	7.92			
Na_2O	4.08		4.24	3.84			
K_2O	.89	.99	.93	.66	.73	.61	1.88
Total	98.49		98.07	99.13			
Trace Elements							
Zn	84		85	75			
Cu	62		56	69			
Ni	18		17	17			
Rb	11		15	12			
Sr	662		673	658			
Co	23		24	18			
Element Ratios							
K/Rb	672		515	456			
Sr/Rb	60.2		44.9	54.8			
K/Sr	11.2		11.5	8.33			
Ca/Sr	80.1		77.4	86.0			
Zn/Cu	1.35		1.52	1.09			

Table 7. (continued)

Major Elements	J15	J17	J18	J20	J22	J23	J24
SiO_2	53.26	64.47	55.61	60.31	63.30	62.00	59.00
TiO_2				.83	.71	.76	.83
Al_2O_3				17.12	17.35	16.07	17.19
Fe_2O_3				6.15	5.33	5.56	6.35
MgO				2.33	2.14	2.11	2.12
CaO				6.42	6.30	6.20	7.09
Na_2O				4.39	4.63	4.39	4.90
K_2O	.54	1.52	.98	.91	1.25	1.44	1.05
Total				98.46	101.01	98.53	98.53
Trace Elements							
Zn				84	73	76	78
Cu				48	32	46	46
Ni				15	15	18	16
Rb				14	17	21	15
Sr				555	533	703	531
Co				10	11	9	12
Element Ratios							
K/Rb				540	610	569	581
Sr/Rb				39.6	31.4	33.5	35.4
K/Sr				13.6	19.5	17.0	16.4
Ca/Sr				82.7	84.5	63.0	95.4
Zn/Cu				1.75	2.28	1.65	1.70

Table 7. (continued)

Major Elements	J28	J30	J32	J33	J35
SiO_2	53.05	48.55	53.16	66.40	58.49
TiO_2				.79	
Al_2O_3				12.74	
Fe_2O_3				5.45	
MgO				2.05	
CaO				6.38	
Na_2O				4.33	
K_2O	.94	.75	1.00	1.58	1.07
Total				99.72	
Trace Elements					
Zn				80	
Cu				44	
Ni				16	
Rb				18	
Sr				701	
Co				7	
Element Ratios					
K/Rb				729	
Sr/Rb				38.9	
K/Sr				18.7	
Ca/Sr				65.0	
Zn/Cu				1.82	

Table 8. Chemical Analyses of Mount Rainier Lava Flows

Major Elements	T04	T06	T08	T14	T17	T18	T20
SiO_2	59.45	62.08	56.64	63.06	58.78	63.78	61.57
TiO_2							
Al_2O_3							
Fe_2O_3							
MgO							
CaO							
Na_2O							
K_2O	1.97	2.03	1.97	2.02	1.68	2.06	1.92
Total							
Trace Elements							
Zn							
Cu							
Ni							
Rb							
Sr							
Co							
Element Ratios							
K/Rb							
Sr/Rb							
K/Sr							
Ca/Sr							
Zn/Cu							

Table 8. (continued)

Major Elements	T24	T31	T32	T34	T35	T37	T38
SiO_2	58.09	58.63	58.78	59.19	60.74	58.89	59.85
TiO_2		.91		.78	.82	.83	.87
Al_2O_3		17.85		17.44	16.87	17.44	16.88
Fe_2O_3		5.77		5.49	5.26	5.88	6.47
MgO		2.46		2.55	2.34	2.55	2.33
CaO		7.08		7.15	6.34	7.25	6.42
Na_2O		4.26		3.43	3.02	3.33	3.13
K_2O	2.08	1.94	2.18	1.86	2.14	1.86	2.15
Total		98.90		97.99	97.53	98.03	98.10
Trace Elements							
Zn		68		92	72	73	68
Cu		36		47	45	37	33
Ni		19		25	19	18	18
Rb		49		62	50	50	51
Sr		500		624	482	482	492
Co		12		12	12	12	9
Element Ratios							
K/Rb		329		269	339	297	350
Sr/Rb		10.2		10.1	9.64	9.64	9.64
K/Sr		32.2		26.8	35.1	30.8	36.3
Ca/Sr				81.9	94.0	107	93.3
Zn/Cu		1.89		1.96	1.60	1.97	2.06

Table 8. (continued)

Major Elements	T39	T40	T41	T43	T44	T46	T48
SiO_2	51.81	53.26	61.33	59.54	60.96	61.00	61.34
TiO_2							.78
Al_2O_3							17.90
Fe_2O_3							5.45
MgO							2.16
CaO							6.93
Na_2O							3.44
K_2O	1.60	1.78	2.14	2.24	2.38	1.98	1.87
Total							99.87
Trace Elements							
Zn							66
Cu							54
Ni							∼
Rb							47
Sr							449
Co							11
Element Ratios							
K/Rb							330
Sr/Rb							9.55
K/Sr							34.6
Ca/Sr							110
Zn/Cu							1.22

Table 8. (continued)

Major Elements	T51	T53	T54	T55	T56	T59	T60
SiO_2	62.27	62.56	59.18	63.01	67.26	62.56	59.65
TiO_2							.84
Al_2O_3							18.00
Fe_2O_3						6.31	5.37
MgO						2.91	2.74
CaO						7.17	6.87
Na_2O						3.21	3.71
K_2O	2.01	2.13	1.95	2.06	2.32	2.12	2.04
Total							99.22
Trace Elements							
Zn						68	75
Cu						56	39
Ni						19	19
Rb						44	53
Sr						488	465
Co						10	13
Element Ratios							
K/Rb						400	320
Sr/Rb						11.1	8.77
K/Sr						36.1	36.4
Ca/Sr							106
Zn/Cu						1.21	1.92

Table 8. (continued)

Major Elements	T61	T62	T63	T64	T65	T67	T68
SiO_2	63.09	64.01	59.87	59.84	60.97	62.30	66.11
TiO_2		.80	.75		.86		.74
Al_2O_3		17.32	17.63		17.31		16.17
Fe_2O_3		5.53	5.40		6.28		4.79
MgO		2.16	2.79		3.04		2.16
CaO		5.97	6.75		6.97		5.90
Na_2O		3.44	3.52		3.52		3.50
K_2O	1.96	1.64	1.60	1.62	1.48	1.70	2.30
Total		100.87	98.31		100.43		101.75
Trace Elements							
Zn		66	69		33		29
Cu		44	33		43		39
Ni		18	18		19		16
Rb		48	42		40		52
Sr		450	476		494		407
Co		10	Tr		Tr		2
Element Ratios							
K/Rb		284	316		307		367
Sr/Rb		9.38	11.3		12.4		7.83
K/Sr		30.2	27.9		24.9		46.9
Ca/Sr		94.8	101		101		104
Zn/Cu		1.50	2.09		.767		.744

Table 8. (continued)

Major Elements	T70	T71	T72	T73	T74	T75	T76
SiO_2	61.25	65.84	63.71	64.88	64.89	66.78	68.62
TiO_2			.83		.69		
Al_2O_3			16.31		16.35		
Fe_2O_3			5.45		4.74		
MgO			2.43		2.18		
CaO			6.06		6.01		
Na_2O			3.92		3.60		
K_2O	1.70	2.37	2.25	2.17	2.31	2.25	
Total			100.96		100.77		
Trace Elements							
Zn			29		32		
Cu			34		36		
Ni			19		29		
Rb			52		50		
Sr			434		403		
Co			Tr		Tr		
Element Ratios							
K/Rb			359		394		
Sr/Rb			8.35		8.06		
K/Sr			43.0		48.9		
Ca/Sr			99.8		106		
Zn/Cu			.853		.889		

Table 8. (continued)

Major Elements	T77	T78	T81	T82	T83	T84	T85
SiO_2	61.82	57.12	62.58	55.04	55.41	55.98	57.36
TiO_2				1.18	1.25	1.14	1.09
Al_2O_3				16.94	17.10	17.28	17.12
Fe_2O_3				9.18	9.45	8.84	8.05
MgO				5.36	5.51	4.71	3.88
CaO				7.83	7.65	7.83	7.42
Na_2O				4.39	3.68	3.92	4.00
K_2O	1.66	1.00	1.91	1.04	.94	1.16	1.40
Total				100.96	100.99	100.86	100.32
Trace Elements							
Zn				30	38	24	92
Cu				41	35	41	42
Ni				24	20	20	11
Rb				22	19	21	29
Sr				496	450	502	527
Co				Tr	Tr	113	121
Element Ratios							
K/Rb				392	411	458	401
Sr/Rb				22.5	23.7	23.9	18.2
K/Sr				17.4	17.3	19.2	22.0
Ca/Sr				113	121	111	101
Zn/Cu				.732	1.08	.585	.621

Table 8. (continued)

Major Elements	T86	T87	T88	R01	R04	R07	R08
SiO_2	57.66	56.75	58.02	63.47	60.22	60.48	64.93
TiO_2	1.09	1.08					
Al_2O_3	16.51	17.87					
Fe_2O_3	8.36	8.02					
MgO	3.81	3.93					
CaO	7.61	7.74					
Na_2O	3.84	3.76					
K_2O	1.17	1.06	.94	1.97	1.79	1.73	1.97
Total	100.32	100.05					
Trace Elements							
Zn	93	79					
Cu	42	43					
Ni	18	24					
Rb	31	29					
Sr	513	515					
Co	110	139					
Element Ratios							
K/Rb	313	303					
Sr/Rb	16.5	17.8					
K/Sr	18.9	17.1					
Ca/Sr	106	107					
Zn/Cu	.645	.724					

Table 8. (continued)

Major Elements	R09	R10	R14	R16	R18	R28	R32
SiO_2	63.06	57.96	59.86	63.01	63.10	65.02	68.40
TiO_2							
Al_2O_3							
Fe_2O_3							
MgO							
CaO							
Na_2O							
K_2O	2.24	1.91	1.72	1.92	2.01	2.20	2.40
Total							
Trace Elements							
Zn							
Cu							
Ni							
Rb							
Sr							
Co							
Element Ratios							
K/Rb							
Sr/Rb							
K/Sr							
Ca/Sr							
Zn/Cu							

Table 8. (continued)

Major Elements	R39	R42	R43	R44	R45	R46	R47
SiO_2	61.96	62.10	62.53	61.39	59.79	58.10	61.28
TiO_2	.82		.82				.85
Al_2O_3			16.38				16.82
Fe_2O_3	5.72		5.30				5.90
MgO	1.94		1.97				2.72
CaO			6.18				6.56
Na_2O	3.68		3.92				3.68
K_2O	2.10	2.16	2.00	1.97	1.57	1.80	2.09
Total			99.10				99.90
Trace Elements							
Zn	69		91				92
Cu	37		33				35
Ni	17		20				12
Rb	49		49				42
Sr	459		472				567
Co	74		73				81
Element Ratios							
K/Rb	356		339				413
Sr/Rb	9.37		9.63				13.5
K/Sr	38.0		35.2				30.6
Ca/Sr			93.6				82.7
Zn/Cu	1.86		2.76				2.63

Table 8. (continued)

Major Elements	R49	R50	R51	R52	R53	R55	R56
SiO_2	61.32	62.33	63.40	63.90	62.53	59.94	54.42
TiO_2	.86		.86		.82	.83	
Al_2O_3	16.61		16.15		15.68	16.16	
Fe_2O_3	5.92		5.81		5.78	5.84	
MgO	2.74		2.36		2.23	2.84	
CaO	6.51		6.12		6.10	6.82	
Na_2O	4.00		4.08		4.16	4.17	
K_2O	2.12	2.15	2.16	2.12	2.04	1.84	
Total	100.08		100.08		99.34	98.44	
Trace Elements							
Zn	93		122		100	121	
Cu	29		39		38	41	
Ni	33		17		18	8	
Rb	46		48		50	56	
Sr	590		481		466	569	
Co	42		27		25	36	
Element Ratios							
K/Rb	378		374		339	273	
Sr/Rb	12.8		10.0		9.32	10.2	
K/Sr	29.5		37.3		36.3	26.8	
Ca/Sr	78.8		90.9		93.6	85.7	
Zn/Cu	3.21		3.13		2.63	2.95	

Table 8. (continued)

Major Elements	R57	R58	R59	R60	R61	R62	R64
SiO_2	54.56	56.68	56.95	55.95	54.54	53.74	53.78
TiO_2							
Al_2O_3							
Fe_2O_3							
MgO							
CaO							
Na_2O							
K_2O	1.42	2.13	1.92	1.90	1.31	1.52	1.44
Total							
Trace Elements							
Zn							
Cu							
Ni							
Rb							
Sr							
Co							
Element Ratios							
K/Rb							
Sr/Rb							
K/Sr							
Ca/Sr							
Zn/Cu							

Table 8. (continued)

Major Elements	R65	R69
SiO_2	55.24	58.04
TiO_2		.86
Al_2O_3		17.91
Fe_2O_3		6.38
MgO		2.25
CaO		7.12
Na_2O		3.96
K_2O	1.12	1.63
Total		98.15
Trace Elements		
Zn		137
Cu		37
Ni		16
Rb		39
Sr		565
Co		23
Element Ratios		
K/Rb		347
Sr/Rb		14.5
K/Sr		24.0
Ca/Sr		90.1
Zn/Cu		3.70

This thesis is accepted on behalf of the faculty of the Institute by the following committee:

Kent C. Condie

Charles E. Chapin

Gale K. Billings

Date March 3, 1974